Long-range modifications of the wind field by offshore wind parks – results of the project WIPAFF

Andreas Platis[1][*], Jens Bange[1], Konrad Bärfuss[3], Beatriz Cañadillas[4], Marie Hundhausen[1], Bughsin Djath[5], Astrid Lampert[3], Johannes Schulz-Stellenfleth[5], Simon Siedersleben[2], Thomas Neumann[4] and Stefan Emeis[2]

[1]University of Tuebingen, ZAG, Environmental Physics, Tübingen, Germany
[2]Karlsruhe Institute of Technology – Institute of Meteorology and Climate Research – Atmospheric Environmental Research, Garmisch-Partenkirchen, Germany
[3]Technische Universität Braunschweig, Institute of Flight Guidance, Braunschweig, Germany
[4]UL International GmbH, Oldenburg, Germany
[5]Helmholtz-Zentrum Geesthacht Zentrum für Material- und Küstenforschung GmbH, Geesthacht, Germany

Abstract

This publication synthesizes the results of the WIPAFF (WInd PArk Far Fields) project. WIPAFF focused on the far field of large offshore wind park wakes (more than 5 km downstream of the wind parks) located in the German North Sea. The research project combined *in situ* aircraft and remote sensing measurements, satellite SAR data analysis and model simulations to enable a holistic coverage of the downstream wakes. The *in situ* measurements recorded on-board the research aircraft DO-128 and remote sensing by laser scanner and SAR prove that wakes of more than 50 kilometers exist under certain atmospheric conditions. Turbulence occurs at the lateral boundaries of the wakes, due to shear between the reduced wind speed inside the wake and the undisturbed flow. The results also reveal that the atmospheric stability plays a major role in the evolution of wakes and can increase the wake length significantly by a factor of three or more. On the basis of the observations existing mesoscale and industrial models were validated and updated. The airborne measurement data is available at PANGAEA/ESSD.

Keywords: WIPAFF, wind energy, offshore, wakes, marine boundary layer

1 Introduction

Wind park wakes have found increasing interest in recent years, when industry and authorities have started to plan wind parks closer together for good reasons (e.g. nature conservation, bundling of grid access, public acceptance), especially in offshore regions. As wind parks are built to extract kinetic energy from the atmosphere, downwind wake regions form behind turbines and wind parks, characterised by reduced mean wind speed and enhanced levels of turbulence (Lissaman, 1979). Both effects downgrade the conditions for downstream turbines and wind parks and are thus relevant for the expected power output from and the endurance of the installations. However, a deeper understanding of the physics of atmospheric flow in wind park wakes is needed to obtain better operational forecasts of wind energy production or scenario simulations (Veers et al., 2019; Rohrig et al., 2019).

We distinguish here between the near wake of wind parks (a few hundreds of metres to a few kilometres behind the parks) where the effects of single turbines are clearly discernible, and the far wake (about five kilometres and more behind the parks) where the wakes of the single turbines have merged into a more or less uniform park wake (e.g. Li and Lehner, 2013a). Most research on wakes so far has focused on near wakes behind single turbines and on wake interactions from a larger number of turbines within one and the same wind park (e.g., Martínez-Tossas et al., 2015; Trabucchi et al., 2015). Only some experimental and recent numerical studies consider the wakes of entire wind parks and the impact of far wakes on neighbouring downwind wind parks on a larger spatial scale (e.g., Chaviaropoulos, 2013; Nygaard and Hansen, 2016; Schneemann et al., 2019).

The impact of far wakes from offshore wind parks on the regional climate has only been addressed in isolated studies (e.g., Boettcher et al., 2015) with hardly any definite conclusions. Recent studies for onshore wind parks found similar effects of the impact Pryor et al., 2018. Wind park far wakes are of particular interest for offshore installations, because turbulence intensity – which is the main driver for wake dissipation – is much lower over the ocean than over land. Therefore, wakes behind offshore wind turbines and wind parks are expected to be much longer than behind onshore wind turbines and parks (see e.g., Barthelmie et al., 2007; Porté-Agel et al., 2020). Analytical studies (Emeis,

*Corresponding author: Andreas Platis, University of Tuebingen, ZAG, Environmental Physics, 72074 Tübingen, Germany, e-mail: andreas.platis@uni-tuebingen.de

2010; Emeis, 2018; Porté-Agel et al., 2020) as well as numerical simulations (e.g. Fitch et al., 2012) have predicted these prolonged wind park wakes as well. Wake lengths up to about 100 km were found in these simulations (Fitch et al., 2012). Observational evidence of such long wakes has been available only indirectly so far from the evaluation of satellite data (Christiansen and Hasager, 2005).

In situ measurements of the far wakes were missing before the initiation of the research project WIPAFF (WInd PArk Far Fields), the main results of which are reported here. WIPAFF has been funded by the German Federal Ministry for Economic Affairs and Energy and ran from November 2015 to April 2019. The main goal of WIPAFF (Emeis et al., 2016) was – for the first time – to perform a large number of *in situ* measurements from aircraft operations at hub height behind wind parks in the German Bight (North Sea), to evaluate further SAR images and to update and validate existing mesoscale and industrial models on the basis of the observations. First results from WIPAFF aircraft operations have been reported by Platis et al. (2018).

This publication is designed to give an integrative overview on the results of WIPAFF. Results from the evaluations of the different measurement and modelling efforts in the project (see Emeis et al., 2016; Djath et al., 2018; Platis et al., 2018; Siedersleben et al., 2018b; Siedersleben et al., 2018a; Siedersleben et al., 2020; Lampert et al., 2020; Platis et al., in review; Djath and Schulz-Stellenfleth, 2020; Cañadillas et al., 2020) are put into a common perspective. The airborne data set of the WIPAFF project is accessible to the community via the PANGAEA database (Bärfuss et al., 2019; Lampert et al., 2020). Section 2 gives the initial hypotheses of the project and Section 3 briefly reviews methods and their state of the art at the beginning of the project. The main results of WIPAFF are summarized in Section 4. Section 5 concludes the study and prepares an outlook to further necessary research.

2 The WIPAFF project's initial hypotheses

Wind turbines generate rotating wake vortices in which wind speed, turbulence intensity and turbulent fluxes are modified compared to the undisturbed flow. In a wind park with many wind turbines arranged in a tight grid, theses single wakes are considered to superimpose each other (Martínez-Tossas et al., 2015; Trabucchi et al., 2015). For the successful planning of further offshore parks, it is therefore crucial to identify the parameters that affect the wake development. There have been some model approaches of varying complexity that simulate these wake processes (Frandsen, 1992; Emeis and Frandsen, 1993; Vermeer et al., 2003; Emeis, 2010; Fitch et al., 2012; Fiedler and Adams, 2014; Volker et al., 2015). A validation, however, of these models has not yet been available so far due to the lack of large offshore wind parks. With the installation of the first large

wind park cluster in the German Bight in the recent decade, this has become possible now. The WIPAFF project aimed to understand the wake development in the lee of wind parks, the corresponding decay dynamics and the size and impact of the wakes downstream of entire offshore wind parks by considering all influencing parameters. In the following, we address the four initial hypotheses of the WIPAFF project.

2.1 Hypothesis 1: Wake appearance is related to atmospheric stability

The most efficient mechanism for wake recovery is the vertical transfer of momentum from higher atmospheric layers downwards by atmospheric turbulence (Emeis, 2010; Abkar and Porté-Agel, 2015a; et al., 2015a; Emeis, 2018). Because of the small surface friction and weak temperature gradients over the sea, much less mechanical turbulence is produced compared to onshore sites (Smedman et al., 1997; et al., 2015b) and, hence, longer wakes are expected. For this reason, surface roughness and atmospheric stability are regarded to be the decisive parameters governing the generation of turbulence and thus the wake recovery (Barthelmie et al., 2009; Barthelmie and Jensen, 2010; Hansen et al., 2012; Wu and Porté-Agel, 2012; Chaviaropoulos, 2013).

Wakes of several tens of kilometres were expected to be especially pronounced at offshore locations during stable conditions (Hansen et al., 2012). This presumption of the existence of far wakes was supported by observational hints of long reaching wakes on satellite images of the sea surface from synthetic aperture radar (SAR, Figure 2). In stable stratifications, long wakes with a length exceeding 20 km have been assessed from synthetic aperture radar data (Christiansen and Hasager, 2005; Li and Lehner, 2013a).

In addition to the fact that stability may play a very important role in the generation of far wakes, studies such as Frandsen et al. (2006); Porté-Agel et al. (2014); Porté-Agel et al. (2013); Barthelmie et al. (2009) showed that the wake intensity within the wind park depends crucially on the wind direction and the park layout. A larger initial wind speed deficit is observed when the wind direction is parallel to the turbine rows and the turbines are aligned. This larger initial wind speed deficit was expected to cause longer wakes according to Emeis (2010).

2.2 Hypothesis 2: Wakes are associated with increased turbulence

Besides the reduction of the wind speed in the wake, turbulent effects, such as high turbulent kinetic energy (TKE) and increased momentum flux were expected. The degree of atmospheric turbulence impacts the efficiency and fatigue loading of a wind turbine (Lee et al., 2012). Two factors were considered responsible for the

production of turbulence. Firstly, the rotating wake vortices by the wind turbines and secondly, the production of turbulence as a result of the mixing of the wake and its decelerated wind field with the undisturbed flow. So far, mesoscale numerical models parameterize wind turbines as elevated moment sinks, and some of them as a source of TKE (BLAHAK et al., 2010; FITCH et al., 2012; ABKAR and PORTÉ-AGEL, 2015b; VOLKER et al., 2015). In large-eddy simulation (LES) studies and wind-tunnel experiments, these effects were determined at a distance of almost 20 times the wind turbine rotor diameter *d* (20*d*) (WU and PORTÉ-AGEL, 2012). However, a validation with *in situ* measurement data has not yet been carried out, except in VOLKER et al. (2015) who used tower measurements collected during neutral conditions to evaluate the wind parks parameterizations of FITCH et al. (2012) and VOLKER et al. (2015).

2.3 Hypothesis 3: Wakes have the potential to impact other wind parks downstream

For an optimal use of the marine areas, wind parks are constructed at favourable locations and in clusters in order to minimize the expense of grid connections and due to other constraints like military zones, pipelines, and nature preserves. However, the close proximity can undermine power production in other wind parks downstream, due to wakes from upwind wind parks, causing an economic loss (KAFFINE and WORLEY, 2010; NYGAARD, 2014; NYGAARD and HANSEN, 2016; BODINI et al., 2017; LUNDQUIST et al., 2019). Simple analytical models and first studies confirmed that especially during thermally stable stratification wakes have an impact on downwind wind parks reducing their efficiency.

2.4 Hypothesis 4: Wakes impact local climate

Large wind farm impose an obstacle in a flat environment, which decelerate the flow locally associated with a flow-around and overflow effects. As a result, the turbulent fluxes and heat in the atmospheric boundary layer (ABL) may change.

It was already known that onshore wind parks can impact the near surface temperature, and the turbulent fluxes of sensible heat, CO_2, and water vapour (latent heat) (e.g. ROY and TRAITEUR, 2010; ZHOU et al., 2012; RAJEWSKI et al., 2013; RAJEWSKI et al., 2014; ARMSTRONG et al., 2016). For example, ZHOU et al. (2012) observed a warming of 0.5 K in the vicinity of onshore wind parks, especially during nocturnal stable conditions. But only a few studies have investigated the potential effect of offshore wind parks on the marine boundary layer (MBL). These studies were motivated by visible cloud effects as they were seen in photos taken at a wind park at the coast of Denmark (EMEIS, 2010; HASAGER et al., 2013; HASAGER et al., 2017), indicating fog formation and dispersion due to enhanced mixing and adiabatic cooling downwind of wind parks. Associated with enhanced mixing, FOREMAN et al. (2017) reported a decreased sensible heat flux downwind of a small offshore wind park during stable conditions in the German Bight by using eddy-covariance measurements of heat and humidity fluxes at the research platforms FINO1 mast.

Also numerical simulations have indicated a change in air temperature and humidity in the downwind direction of offshore wind parks. VAUTARD et al. (2014) identified increased temperatures in the area of offshore wind parks in their simulations, whereby WANG and PRINN (2011) reported a potential cooling effect in the vicinity of offshore wind parks due to an increased latent heat flux. These thermal effects were not investigated by field measurements, so far. Therefore, in the framework of the WIPAFF project, their spatial extent was investigated together with the possibility that larger wind parks may have an influence on the local climate.

3 Methods used in the WIPAFF project

3.1 Airborne Data

Airborne *in situ* data were collected with the research aircraft Dornier DO-128 operated by the Technische Universitat Braunschweig, Germany. 41 measurement flights over the German Bight during the WIPAFF project during 2016 and 2017 delivered (in general at a sampling frequency of 100 Hz) 3D wind vector, temperature, humidity, and sea surface-temperature. A detailed explanation of the used measurement instruments and the aircraft can be found in CORSMEIER et al. (2001); PLATIS et al. (2018); LAMPERT et al. (2020). The starting points of the flights were Wilhelmshaven, Borkum or Husum airport, respectively. A typical flight pattern to capture the wakes is displayed in Figure 1 is the so-called "meander pattern", with several flight legs at hub height (at about 100 m above sea level) positioned downstream of the wind-park cluster. The data is freely available from BÄRFUSS et al. (2019) and further explained in LAMPERT et al. (2020).

Besides the meteorological *in situ* data, a downward-looking scanning lidar system measuring the distance aboard the research aircraft recorded the sea-surface state for deriving the shape and distribution of the sea waves, and for characterizing the far-field wakes.

3.2 Satellite information for retrieving surface properties

Active microwave radar sensors such as Synthetic Aperture Radar (SAR) are powerful instruments for sunlight and weather independent measurements of the ocean surface roughness at high spatial resolution. The capability of SAR to provide information on offshore windpark wakes has been amply demonstrated (CHRISTIANSEN and HASAGER, 2005; LI and LEHNER, 2013a; DJATH et al., 2018). Far field wake effects of more than 10 km downstream of offshore wind parks have for the
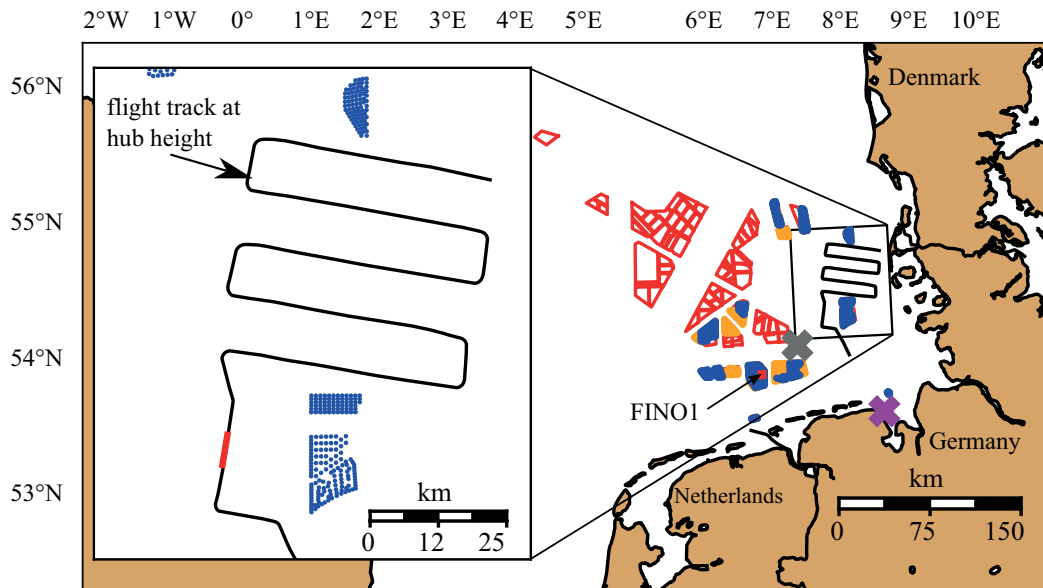
Figure 1: Distribution of offshore wind parks in the German Bight as of December 2017. Blue regions are parks currently in operation, red indicate parks still in the approval process. Orange regions are those wind parks that are under construction. The red line within the close-up indicates the area where typically the vertical profiles where flown to capture the atmospheric stratification in close vecinity to the wind farm. The map is adapted from data of the German Federal Maritime and Hydrographic Agency (BSH) and adapted from PLATIS et al., 2018. The magenta and grey colored crosses show locations of climb flights as indicated in Figure 16.

first time become evident based on the analysis of SAR images (CHRISTIANSEN and HASAGER, 2005; LIN et al., 2008; LI and LEHNER, 2013b). In the WIPAFF project, SAR revealed changes of surface properties downwind of wind parks, expanding the airborne observations to a scale beyond 100 km.

SAR measures near surface wind fields in an indirect way through the small scale roughness of the sea surface. The wind influences the sea surface by generating cm-scale roughness, which is captured by active microwave sensors due to the Bragg-scattering principle. Low image intensities thus indicate areas of reduced wind speed.

Sentinel-1A (launched in 2014) and Sentinel-1B (launched in 2016) are twin satellites that provide SAR data in the German Bight on a regular basis. They were launched into a sun-synchronous orbit and operate at C-band (5.405 GHz) at vertical receive and transmit polarization (VV). Each satellite has an exact repeat cycle of 12 days for the same imaging geometry (i.e., incidence angles and area covered are identical), but can provide data for a particular spot at one or two day intervals, if different imaging geometries are acceptable. Thus, the combination of both satellites provide an image every 6 days with identical geometry. The estimation of wind speeds from SAR requires the radiometric calibration of the SAR raw data and the inversion of a so called geophysical model function (GMF) (HERSBACH et al., 2007; VERHOEF et al., 2008). Wind direction information can be retrieved either from SAR image structures or alternatively external sources (e.g., atmospheric models) are used.

Wind speed deficits were estimated from SAR using a technique proposed in CHRISTIANSEN and HASAGER (2005) and a new filter approach described in DJATH and SCHULZ-STELLENFLETH (2020). The overall challenge in this application is the estimation of the undisturbed background wind speed, which is not available at the exact location of the wake. The use of wind speeds in neighbouring areas as a proxy leads to certain errors, which depend on spectral properties of the background wind field and which are discussed in more detail in DJATH and SCHULZ-STELLENFLETH (2020).

A spectral analysis of wind fields in the German Bight was conducted as follows. SAR scenes from both satellites were collected for the period September 2016 to December 2017. The occurrence of wakes around the wind park Amrumbank West was analysed (Figure 1). Only the scenes that included the entire Amrumbank West were considered and overall, 177 scenes were collected. Wave-number spectra were then computed from the SAR derived 10 m-wind speed maps. Wind field data were classified considering the stability conditions based on the thermal stratification from FINO1 data. Wind fields associated with stable conditions (STA) and unstable conditions (NOSTA) were considered. A 2D spectral analysis was applied to a square box of 320×320 grid points (with a grid spacing of 300 m, i.e. spatial resolution) aside the wind turbines (see blue box in Figure 2). Using this area, a wavelength range between 0.6 km and 100 km is covered. A 2D Fast Fourier Transform (FFT) was applied to the SAR derived wind fields after the mean was removed. The resulting 2D wavenumber spectrum was scaled in

such a way, that integration of the entire spectral domain equalled the total variance of the wind field. As the wavenumber and directional dependency were also analysed, the spectra were interpolated from the original 2D Cartesian grid to a polar grid. The 1D spectrum was then computed by integrating over all directions.

Besides the observational data, different (numerical) model types were used to investigate the far field of offshore wind parks.

3.3 Mesoscale model and wind-park parameterizations (WPPs)

All mesoscale numerical simulations were performed with the Weather Research and Forecasting Model WRF (version 3.8.1). We used the wind park parameterization of FITCH et al. (2012) to simulate the wakes of offshore wind parks in the German Bight. Wind park parameterizations (WPPs) allow one to simulate the impact of several wind parks on the marine boundary layer due their low computational costs. Nowadays, offshore wind parks cover an area on the order of $100\,km^2$ and the corresponding wakes exceed $50\,km$ downwind (Figure 2). Consequently, large offshore wind parks affect a large area, hence, high resolution large-eddy simulations covering the wake area and the corresponding wind park are computationally too expensive to estimate the economic potential loss of planned offshore wind parks or the regional climate impact of wind parks. For such purposes, WPPs are a suitable tool.

The wind park parameterization of FITCH et al. (2012) extracts momentum from the mean flow at the rotor area and adds TKE at rotor height. In contrast, others (e.g. JACOBSON and ARCHER, 2012; e.g. VOLKER et al., 2015) do not add any TKE as they assume that the TKE develops due the resolved shear. However, both approaches simulate wakes of offshore wind parks with a length exceeding $50\,km$ during neutral conditions (VOLKER et al., 2015).

Evaluation studies testing the performance of WPPs for offshore wind parks during stable conditions are rare. HASAGER et al. (2015) compared SAR retrieved wind speed to mesoscale simulations. VOLKER et al. (2015) tested their WPP and that of FITCH et al. (2012) with real case data using idealized simulations. However, all these evaluation studies were either based on remote sensing data allowing only an evaluation of the wind speed $10\,m$ above mean sea level (msl) or on idealized simulations omitting moisture effects and assuming a stationary inflow. Therefore, studies investigating the performance of WPPs for real case simulations are necessary.

3.4 Analytical model

Analytical wind park models for the assessment of wakes can be constructed in two ways. These models are either bottom-up models which are based on overlays of several single-turbine wakes (the description of which

dates back to JENSEN, 1983) or they are top-down models which consider wind parks as a whole, e.g., as an additional surface roughness, as an additional momentum sink or as a gravity wave generator in association with a temperature inversion aloft at the top of the boundary layer (for the latter idea see SMITH, 2010), which modifies the mean flow above wind parks (NEWMAN, 1977; BOSSANYI et al., 1980; FRANDSEN, 1992). Such models have analytical solutions which make them attractive, although they necessarily contain considerable simplifications. Nevertheless, they can be used for first-order approximations in wind park design. Furthermore, a significant advantage of top-down models that they implicitly include the 'deep array' effects (BARTHELMIE and JENSEN, 2010). Wind turbines in a large array influence the flow in the atmosphere above the wind farm (CHAMORRO and PORTE-AGEL, 2011). It has been proposed that this prevents the entrainment of momentum from the air above the wind farm, restricting the wake recovery (NYGAARD, 2014).

The analytical wind park model of EMEIS (2010) is an extension of earlier ideas documented in FRANDSEN (1992) and EMEIS and FRANDSEN (1993). An updated version which additionally includes the turbulence generated by the turbines in the wind park itself is documented with all equations in Chapter 6 of EMEIS (2018). The basic idea of this model is that the overall momentum consumption of the turbines in very large wind parks, which is proportional to the drag coefficient of the turbines and the wind speed at hub height, can only be compensated for by a turbulent momentum flux from above. This leads to an analytical equation for the reduced horizontal wind speed at hub height in the interior of large wind parks. In the wake behind such large wind parks the wind speed at hub height can only recover again due to a turbulent momentum flux from above. This leads to an exponential function for the wind speed recovery at hub height in the wake. The length of the wake is arbitrarily defined as the distance behind the wind park where the wind speed has recovered to more than $95\,\%$ of the undisturbed value ahead of the wind park. We note that the decay coefficient used here is not the wake decay coefficient (WDC) used in the quadratic decay function of JENSEN (1983). In this analytical model the wind speed reduction at hub height within a large wind park is given as a function of the areal density of turbines in the park, (sea) surface roughness, turbine-induced turbulence and the thermal stability of the atmospheric boundary layer. The wake length in the analytical model depends on the reduced wind speed right after the wind park and the latter three parameters mentioned before. The park layout, i.e., the spatial arrangement of turbines within a wind park, is not covered by this analytical model.

3.5 Engineering models

Engineering models are widely used in the wind energy industry due to their low computational costs and ease

of use to account for wind park wakes. Direct wakes of each individual turbine are simulated with the 'modified PARK' model (KATIC et al., 1987). Alternatively, the 'Eddy Viscosity' model AINSLIE (1988) could be used. Experience shows that the differences between the two models are particularly relevant in the first kilometers behind the wake-generating turbine. Since in the WIPAFF context, however, the effects beyond 10 km on the lee side of the wind park are particularly relevant, the 'modified PARK' model is used here due to the significantly shorter computing time.

In large (offshore) wind parks, the turbines cannot be regarded as independent of the free wind field. Rather, they extract momentum from the wind and therefore act like an area with increased roughness. This results in the formation of an internal boundary layer (IBL) with reduced wind speed behind each turbine. The exact shape of the IBL and the resulting wind speed reduction depends on the orientation of the wind park layout relative to the wind direction (DNV-GL, 2013a).

Both (the 'modified PARK' model combined with an IBL) together allow a reasonable simulation of the wake in offshore wind parks and wind park clusters and are often used in this combination for the determination of wind park yields. Importantly, as the individual turbine wake and IBL models have been developed assuming neutral conditions, stratification needs to be explicitly accounted for by tuning the parameters of these models to match the observations (PEÑA and RATHMANN, 2014) and to get an accurate estimation of energy production.

4 Results

In the following the four hypotheses described in Section 2 are tested.

4.1 On hypothesis 1: Wake Appearance

4.1.1 Appearance of wakes from SAR and airborne data

28 out of the total 41 flights during the WIPAFF project included a flight strategy which allowed for the determination of wakes behind wind parks. For 12 out of the 28 flights, the wake length, defined as the distance to 95 % recovery of the wind field, exceeded the length of the flight meander pattern and for two flights the wake length was observed to be shorter than the downwind distance of the first measured leg. The observed wakes within the WIPAFF campaigns range from nearly 0 km in unstable atmospheric conditions to over 65 km in atmospheric stable conditions (see for further results and discussion Section 4.1.2). The flow inside the wakes was reduced up to 43 % compared to the undisturbed flow, two examples are shown in Figure 4 and 10a).

In addition to the airborne observations, wakes were identified by the analysed surface roughness and backscatter signal (Normalized Radar Cross Section –
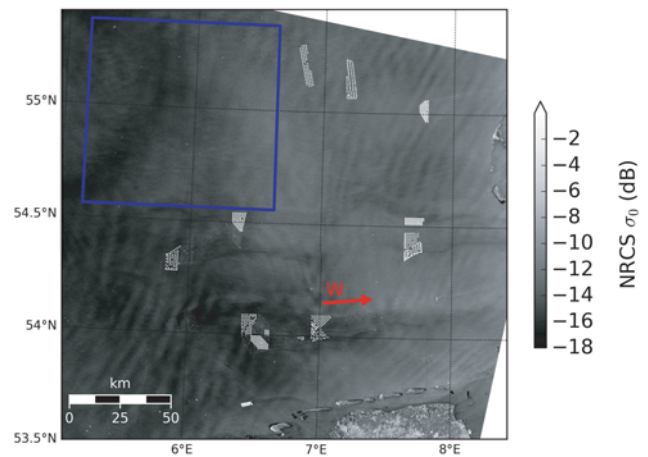

Figure 2: NRCS from Sentinel-1A acquired on 27 May 2019 at 05:49 UTC (Copernicus Sentinel data [2019]). Dark streaks in East-West direction behind the wind parks represent atmospheric wakes. Strong atmospheric related NRCS modulation are also found in North-South direction. The blue box was used for the estimation of 2D wavenumber wind spectra. The red arrow indicates the wind direction.

NRCS) from SAR Sentinal – 1A and 1B observations, e.g. Figure 2. The images exhibit darker streaks downwind of wind parks and brighter features at the edges of the wakes, which indicate that surface roughness is reduced downstream of wind parks, and increased along the edges of the wind parks. An example of recent Sentinel-1A SAR image on 27 May 2019 in Figure 2 shows the wakes through the east-west oriented dark streaks behind the wind parks and are in line with the wind direction coming from West. The wind direction is given by the German weather service (DWD) that provides hourly weather data. The wake behind individual wind parks are longer than 30 km. Statistical analysis from SAR data and atmospheric stability by DJATH et al., 2018 showed wakes longer than 50 km and also revealed that the wakes are longer for stable conditions. Overall, from the total 177 collected scenes between 2016 and 2017, 38 % of them show wakes downstream of offshore wind parks. The case with missing wakes on SAR could be related to either strong atmospheric instability or the fact that the wind farms are not in operation.

4.1.2 Longer wakes during stable stratification

Experimental observations by SAR and aircraft indicated that the wake length depends on the stability of the surrounding atmospheric flow. Therefore, a detailed correlation analysis was performed in order to quantify the effect of different stability definitions on the wake length.

A layer is considered as stable, when vertical motion is suppressed, and as unstable or convective, when vertical motion is enhanced (STULL, 2012). By theory and as outlined in EMEIS et al. (2016), it is typical over the ocean for the northern hemisphere in the temperate west-wind belts that warm sector winds most fre-

quently come from the south-west and thus are followed by rather stable conditions, whereas cold-sector winds come from the north-west and predominantly bring convective conditions. For the German Bight, long term studies conducted during recent years support these assumptions (WESTERHELLWEG et al., 2010; SATHE, 2010; MUÑOZ-ESPARZA et al., 2012; EMEIS et al., 2016).

A common stability parameter is the static stability or lapse rate γ, which takes solely buoyancy into account. The lapse rate is defined by the derivation of the virtual potential temperature θ_v with respect to the vertical coordinate z, and can be approximated by the temperature difference $\Delta\theta_v$ between two levels separated by height difference Δz:

$$\gamma = \frac{d\theta_v}{dz} \approx \frac{\Delta\theta_v}{\Delta z} \quad . \tag{4.1}$$

Thus, γ is negative during convective conditions and positive for stable cases.

Common parameters that express dynamic stability, considering both buoyancy and shear, are the Obukhov length and the bulk Richardson number (STULL, 2012; MUÑOZ-ESPARZA et al., 2012). Moreover, there are measures of the magnitude of turbulence, not considering any thermal stratification at all. Most common in ABL science is the turbulence kinetic energy (TKE) per volume and unit mass

$$k = \frac{1}{2} \cdot \left(\overline{u'^2} + \overline{v'^2} + \overline{w'^2} \right) \tag{4.2}$$

taking the turbulent part of the wind speed components into account.

We used SAR and flight data in the WIPAFF project to investigate the correlation between stability and wake length.

In a first step SAR scenes taken over the offshore windpark Alpha Ventus were analysed and wake lengths were estimated using the technique described in CHRISTIANSEN and HASAGER (2005). This technique consists of estimating the velocity deficit from two parallel transects defined such that one transect encloses the wake area and the second transect is defined outside the wake, which is characterised as freestream conditions. The length at which the wind speed inside the wake has recovered to the freestream characterizes the maximum length of the wake. The scenes were collocated with estimates of the vertical gradient of potential temperature obtained from the nearby FINO-1 platform. The vertical gradient is based on the measurement of the hourly sea surface temperature at FINO1 and the air temperature at 50 m height. The resulting scatter plot is shown in Figure 3. One has to emphasize that this analysis only includes measurements during the early period (2011–2015), where the Alpha Ventus windpark was not affected by neighbouring wind farms, like it is today. One can clearly see a relationship between increasing atmospheric stabilities and growing lengths of the offshore wind farm wake. More details are given in DJATH et al. (2018).
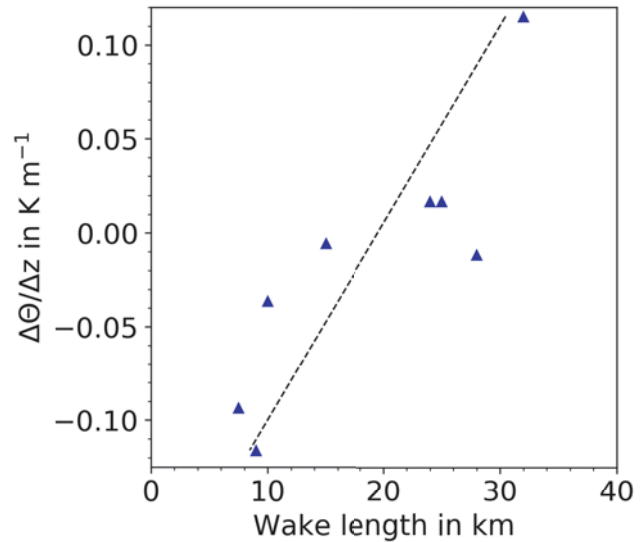

Figure 3: Scatterplot of SAR derived wake lengths versus atmospheric lapse rate $\gamma = \frac{\Delta\theta_v}{\Delta z}$ derived from FINO-1 data (adapted from DJATH et al. (2018)).

The second data source for the determination of the stability were the airborne measurements. We used the vertical profiles obtained during the WIPAFF measurement flights close to the wind parks as marked in Figure 1 for the stability estimation. Further, to examine the relationship between wake expansion and stability, the wake length obtained from flight data (e.g Figure 4) was compared to the stability parameters such as L, $\mathrm{Ri_B}$, and γ. However, a general statement is difficult. Most promising results were achieved using γ (Figure 5a), using a height interval Δz from the uppermost position of the wind turbine blade tip (at 150 m agl for the Amrumbank West wind park AW, for instance) to the lowest position (at 30 m agl for AW). Thus, the height interval covers the entire rotor area, as this was assumed to be the most representative height interval with respect to the wake origin.

Looking at the distinct wind park clusters (Figure 5), the correlation between wake length and stronger stability, as observed for the wind parks GO (Godewind) and AW, can be approximated by two different exponential functions. This is an indication that there are more parameters that govern the wake length, in addition to stability – possibly also the wind-park architecture as considered in the analytical model. Moreover, strong stability coincides with the absence of short wakes. In addition, there is a correlation between higher wind speed deficit with more stable atmospheric conditions (not shown), while small wind deficits occur during more convective conditions.

Using the airborne data set of the WIPAFF project, a distinct correlation between the wake length and the other stability parameters L and $\mathrm{Ri_B}$ (not shown) was not apparent. Summing up, the correlation analysis for wake length and stability exhibits large uncertainty and data scatter. A major problem is the exact determination
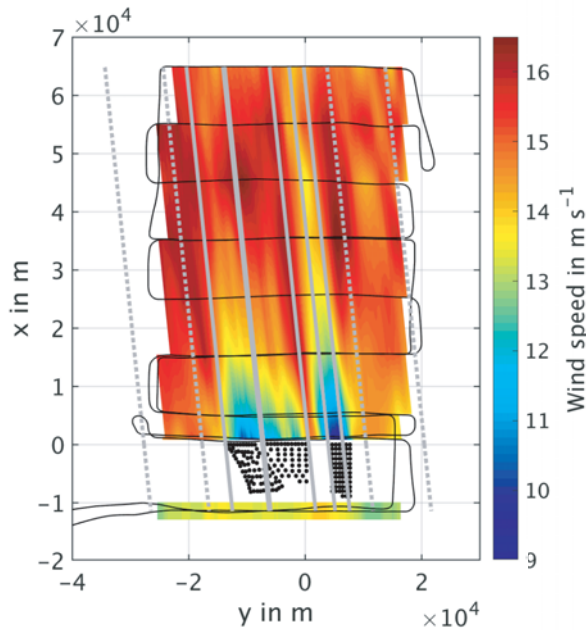
Figure 4: Contour plot of the interpolated wind field, measured during Flight 31 on 08 August, 2017, including the indication of the undisturbed wind field (grey dashed lines) and the wake boundaries (grey solid lines). The black line refers to the flight track (so-called "meander pattern"), black dots indicate the wind turbines of the wind park cluster Amrumbank West, Nordsee Ost and Meerwind Süd/Ost. The mean wind direction is from the east. The top of the map is oriented towards the west. Adapted from PLATIS et al. (in review).

Figure 5: Scatter plots of the wake length versus lapse rate $\gamma = \frac{\Delta \theta_v}{\Delta z}$ obtained from the flight measurement. The according wind park is colour coded. Wakes were measured downstream of the wind parks Amrumbank West (AW), Nordsee Ost (NO), Meerwind Süd/Ost (MSO), Godewind (GO). Cluster implies that only one single wake was identified downstream of the wind park cluster consisting of the wind parks AW, NO and MSO. The regression lines (Reg.) are color coded with respect to the color of the respective wind farm cluster. The regression line is plotted is blue for the wind farm GO green and for the AW. In the case the wake length exceeds the coverage of the flown meander pattern (cf. Figure 4), the non-filled marker is used for the minimum measured wake length.

of stability. A variation of e.g. the height interval for the lapse rate γ or the occurrence of an inversion below the hub height (cf. Section 4.1.3) changes the results significantly. A more detailed analysis will be shown in a following study.

4.1.3 Vertical Structure of wakes

The vertical structure of the atmospheric boundary layer approaching the wind park has a decisive impact on the wake forming. Especially the occurrence of temperature inversions is important. The aircraft data documented several cases where the inversion was either below, at the rotor area of the turbines, or above (SIEDERSLEBEN et al., 2018b). In each of these cases a different behaviour of the wake could be observed. The main challenge with inversions near to or at hub height is that the thermal stratification of the atmospheric boundary layer and the respective level of turbulence are different below and above the inversion. This makes it very difficult to assign a specific thermal stratification to an observed wake development. An inversion below the rotor area decouples the wake development from the state of the sea surface. An inversion above the rotor area prevents the wake from spreading into higher parts of the boundary layer. Inversions are quite common above the North Sea, especially if the flow comes from land upstream. Internal boundaries form when the flow transits across the shoreline from land to water (see, e.g., SMEDMAN et al., 1997).
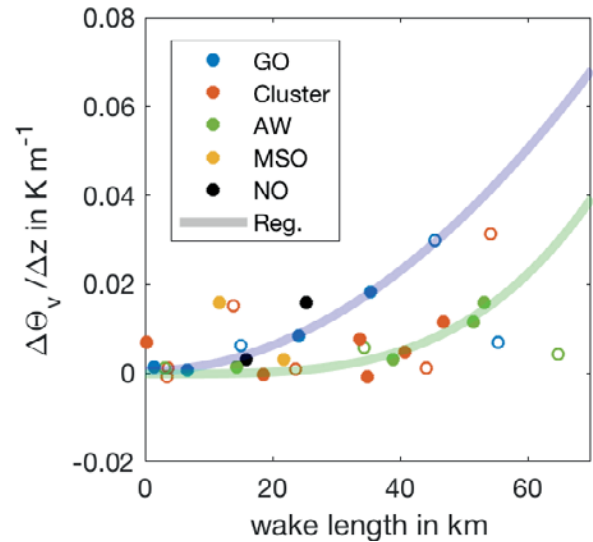
Given the distance of the North Sea wind parks from the coast the top of this internal boundary layer is very often found in the height range of the rotor area (LAMPERT et al., 2020). There are not only newly-formed inversions at the top of internal boundary layers but also inversions advected from the land upstream where they had formed due to radiative cooling in the nocturnal boundary layer. If these cold near-surface layers are advected over warmer sea water, the layer underneath the inversion can be turned into a neutral or even slightly unstable layer while the stratification above the inversion remains more or less unchanged. The propagation conditions for wind park wakes may be further complicated by jet-like wind maxima at the top or just above the internal boundary layer (see, e.g. SMEDMAN et al., 1996). The variety of different vertical profiles of potential temperature and wind speed from 26 aircraft operations in WIPAFF is documented in SIEDERSLEBEN et al. (2018b); LAMPERT et al. (2020) while a case study from one flight is presented in SIEDERSLEBEN et al. (2018a). It is not only the propagation of the wake which is determined by the vertical structure of the air approaching the wind parks but the vertical structure also determines whether the air at hub height behind the wind park is warmer or cooler than before. Figure 6 shows a schematic of this dependence. An inversion in the upper part or just above the rotor area associated with turbulent vertical
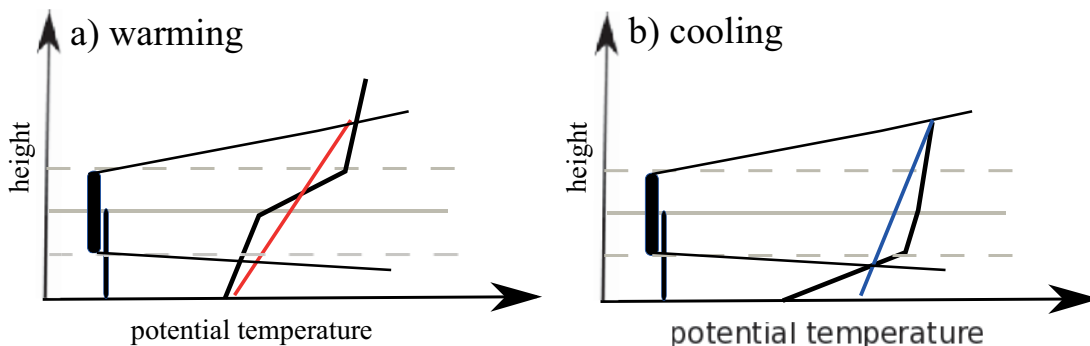
Figure 6: Schematic of stability-dependent temperature change at hub height in wind park wakes (left: warming, right: cooling). Bold vertical line: rotor disk, cone-like structure: wake, black vertical profile: initial temperature profile, red and blue curves: temperature profiles modified by the wake. (From SIEDERSLEBEN et al., 2018b)

mixing within the wake results in a warming of the air at that height. In contrast, an inversion in the lower part or just below the rotor area results in a cooling of the air at that height. In a constantly stable boundary layer without inversions turbulent mixing within the wake will lead to warming below hub height and cooling above hub height. This warming below hub height is similar to satellite observations of nocturnal surface warming behind onshore wind turbines (see, e.g. XIA et al., 2017 and references therein). Nevertheless, the observed temperature changes are merely a vertical re-distribution of heat by the additional turbulence in the wake.

4.1.4 Wakes covered by mesoscale and industrial models

The numerous observations of wakes allowed the evaluation of wake simulations. Within the WIPAFF project, two kind of simulations were evaluated. First of all, mesoscale simulations using WRF and the wind park parameterization of FITCH et al. (2012) were compared against the airborne observations. Secondly, we tested the ability of commonly used industrial models to capture wakes of large offshore wind parks during stable conditions. In this overview paper we focus on observations covering simulations of a wake event observed on 10 September 2016 during atmospheric stable conditions and moderate wind speed of around $8.5 \, \mathrm{m \, s^{-1}}$.

The WRF simulations captured the horizontal dimensions of the wake but overestimated the vertical extent (SIEDERSLEBEN et al., 2018a). The wake observed on 10 September 2016 extended more than 45 km downwind of the wind park Amrumbank West, agreeing with the simulations PLATIS et al., 2018. However, the vertical extent of the wake was overestimated in the simulations. For example, a wind deficit in the order of 5 %–10 % was observed 5 km downwind of the last turbines of Amrumbank West at 200 m above MSL. In contrast, a wind deficit on the order of 20 % and 15 % was simulated (not shown).

The simulated wind speed upwind of the wind parks was $1.5 \, \mathrm{m \, s^{-1}}$–$2 \, \mathrm{m \, s^{-1}}$ too low SIEDERSLEBEN, 2018a. Consequently, the wind speed within the wake of
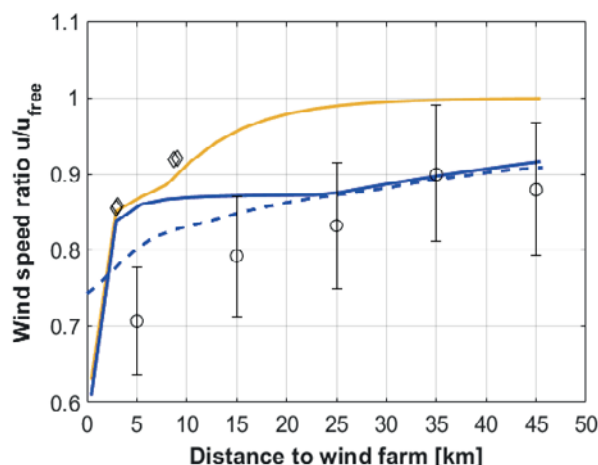

Figure 7: Wind speed reduction relative to free wind speed (10 m/s) in the wake of the wind park cluster Amrumbank/North Sea Ost/Meerwind on 10 September 2016. Shown are the flight data (black dots with error bars), the WRF simulation (blue dashed line), as well as two wake simulated with WindFarmer: default settings (orange solid line) and adjusted settings (blue solid line) the diamonds correspond to the original measurements used to calibrate the default WindFarmer set-up DNV-GL, 2013b.

the simulations was underestimated as well (Figure 7). Aircraft vertical profiles of the atmosphere obtained by climb flights revealed that the simulated stratification of the atmosphere was too unstable at the transition area from land to open ocean. Therefore, we suggest that the overestimated vertical extent of the simulated wake is rooted in a wrongly simulated stratification of the atmosphere.

To compare the WRF simulation and the industrial model (WindFarmer Version 5.2.11 was used within the project) with the flight measurements, a methodology similar to that described in CAÑADILLAS et al. (2020) was used to extract the minimum value of the wind speed along the wake centerline. Layouts and turbine types were chosen identical to those used in the WRF simulation. In WindFarmer, the model options "modified PARK" and "IBL" (internal boundary layer) were selected. This combination is based on the best repre-

sentation of the park effects in offshore wind parks and clusters to determine park yields. While the wind speed deficit in the modified PARK and Eddy Viscosity models decreases with increasing turbine spacing, this is not the case in the IBL implementation, which is of course unphysical. The recovery of the wind velocity deficit from the IBL model was therefore realized by an additional function (so-called "wake recovery function"). Downstream of the wind farm, the wind speed recovery is modelled explicitly as a power function DNV-GL, 2013a

$$U_R(x) = 1 - \left(1 - \frac{U}{U_\infty}\right) 0.5^{\left(\frac{x - x_{\text{start}}}{x_{50\%}}\right)}, \qquad (4.3)$$

where x_{start} is the downstream distance specifying the start of the power function, and $x_{50\%}$ is the location where the wind speed recovery U_R has recovered to half its initial value.

The standard parameterization of the wake recovery function starts at $x_{\text{start}} = 60D$ (D is the rotor diameter; here $D = 120$ m) behind the turbine and after another $x_{50\%} = 40D$ has reduced half of the wind speed deficit. These values were derived by WindFarmer from mast measurements at the lee side of the Danish wind parks "Horns Rev" and "Nysted". With this parameterization the wake curve (orange solid line) is obtained by DNV-GL, 2013b, which is shown in Figure 7. Apparently the wind speed recovers much faster with this parameterization than measured by the research aircraft on 10 September 2016.

A more detailed analysis shows that the measuring masts at "Horns Rev" and "Nysted" are each installed east of the parks, so that the park wake there can only be determined with westerly winds. It is known from stability studies conducted at the offshore mast FINO1 that neutral to stable stability conditions dominate in westerly winds (EMEIS et al., 2016). Probably the parameters for the wake recovery function in WindFarmer were determined on the basis of neutral to unstable stratifications. By contrast, neutral to slightly stable conditions prevailed on 10 September 2016.

It is known from the observations in WIPAFF (CAÑADILLAS et al., 2020) and from the analytical wake model of Section 4.1.5, that considerably larger wake lengths result with stable atmospheric stratification compared to neutral and unstable stratification. This supports the assumption that the wake length differences between the measurements and the standard parameterization in WindFarmer are mainly due to an incorrect accounting of stability effects in the default set-up of Wind Farmer. However, the measurements can be well reproduced by a different parameterization (start of wake recovery at 200D, 50 % recovery after another 200D) for distances beyond 22 km from the wind park cluster (Figure 7). For further discussions, please refer to CAÑADIL-LAS et al. (2020).

4.1.5 Wake Decay Formula

Besides the numerical models, a simple analytical model approach to determine the wake length and wind speed recovery was validated based on the flight data collected during WIPAFF PLATIS et al., in review. The analysis of several different case studies (Figure 8) suggests that the recovery in terms of the wind speed ratio (wake wind speed to undisturbed wind speed at hub height) can be characterized by an exponential function as expected from the analytical model described in EMEIS (2010); EMEIS (2018).

The advantage of the model is that the spatial behavior of the reduced wind speed $u_r(x)$ in the wake at the downstream distance x is described in a single equation. It solely depends on the initial wind speed deficit u_{r0} directly downstream of the wind farm and the wake recovery rate α.

$$u_r(x) = u_f + (u_{r0} - u_f) \exp(-\alpha x) \qquad (4.4)$$

where u_f is the undisturbed (free) wind speed (outside the wake) at hub height. The wake recovery rate α is

$$\alpha = \frac{K_m}{(\Delta z)^2}, \qquad (4.5)$$

where K_m is the momentum exchange coefficient. The height $z = h + \Delta z$ describes the height where the undisturbed wind speed is reached above the wind farm.

By testing the analytical model against the airborne data set, we showed in PLATIS et al. (in review); CAÑADILLAS et al. (2020) that the analytical model performs very well as a first-order approximation. This strengthens the hypothesis that the vertical downward momentum flux is the dominating factor for the wake recovery. Best agreement of the exponential wake recovery curve with the observations was achieved for the case study for Flight 31 (Figure 4). The wind data was extracted based on the method described in PLATIS et al. (in review) and plotted in Figure 8, showing the relative wind speeds between the wind speed in the wake and the undisturbed speed behind several wind farms during which stable and homogeneous conditions prevailed. Further results are discussed in detail in PLATIS et al. (in review); CAÑADILLAS et al. (2020).

A drawback of the analytical model is the determination of the separation height between the hub height and the undisturbed flow above the wind park which must be specified in order to determine the decay coefficient in the exponential wake recovery relation as already noted by PEÑA and RATHMANN (2014). It is also expected, that Δz might not be constant along the wake. Further, the impact of the park layout on the intensity and length of the wake is only covered by the analytical model through the initial deficit. Apart from that, the decay coefficient in the analytical model does not depend on the turbine-induced turbulence left over from the wind park, but only on the upstream conditions. As expected by PORTÉ-AGEL et al. (2020) a modification of
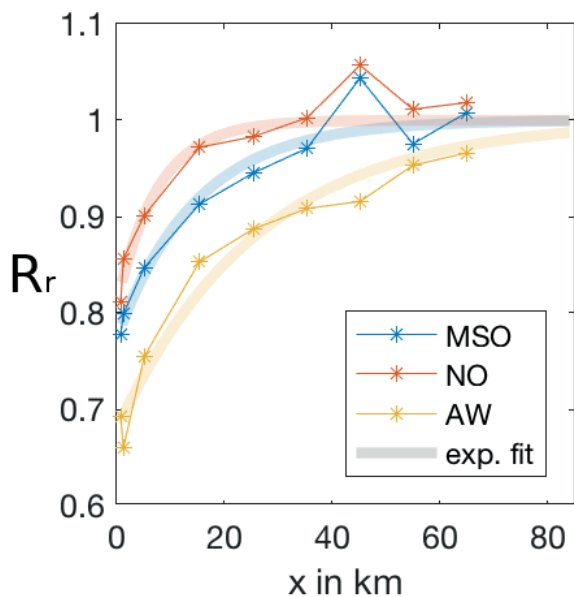
Figure 8: Wind speed ratio $R_r = \frac{u_r}{u_f}$ between the wind speed inside (u_r) and outside the wake (u_{un}) of flight 31 on August 8, 2017. Dots indicate the measured ratios $R_r = \frac{u_r}{u_{un}}$ and the line the exponential fit according to the analytical model. Blue indicates the wind speed analysis in the wake downstream of the wind farm Meerwind Süd/Ost (MSO), red Nordsee Ost (NO) and yellow Amrumbank West (AW). Adapted from PLATIS et al. (in review)

a)

b)

Figure 9: Normalised radar cross section (a) associated with sea surface roughness as derived from a Sentinel-1B image acquired on 18 June 2017 at 05:48 UTC (Copernicus Sentinel data [2007]) and derived near surface wind speed (b) showing an increase of NRCS and wind speed within the first 10 km downstream Sandbank (wind park on the left) and DanTysk (wind park on the right) wind parks. The red arrow indicates the wind direction.

the atmospheric stability (e.g u_*) by forming a farm-induced internal boundary layer (IBL) is likely and has to be considered in further editions of this model.

4.1.6 Wakes change the sea surface

Wakes downstream wind parks are visually detectable on SAR images and usually characterized by dark streaks in line with wind direction (Figure 2). However, some images show brighter areas (increase of NRCS and thus wind speed) within the first 10 km downstream the wind parks. An example of an increase of NRCS downstream of the wind park is shown on Figure 9 acquired on 18 June, 2017 at 05:48 UTC during stable stratification (air temperature is 16 °C, while SST is 15.4 °C). This leads to an inferred increase of wind speed in Figure 9b, which is an unusual behavior. The mechanism of this behaviour is unknown. Nevertheless, a theoretical model was proposed in DJATH et al. (2018), which tried to explain this atypical observation by an increased downward momentum flux associated with increased turbulence generated by the wind park. Indeed, the turbulence, which is generated mechanically by the wind turbines, leads to an increase of friction velocity and radar cross section. The turbulence slowly dissipates downstream and after some distance the downward momentum flux is not effective any more. Mechanisms of this kind can be expected to be most effective in atmospheric stable stratification with strong vertical wind speed gradients. The SAR observations are confirmed by airborne laser scanner observations: Within the wake,
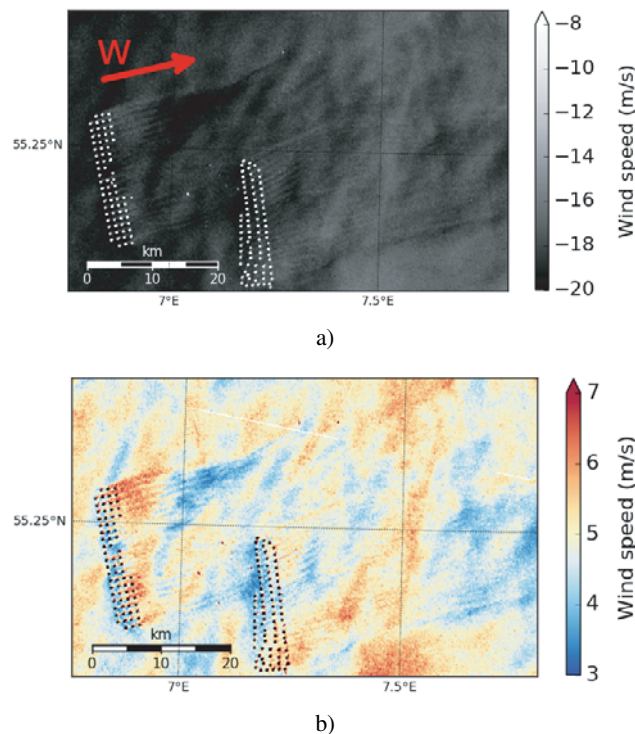
the reflectance is significantly enhanced (Figure 10c). An explanation is the flatter surface, which reflects back more energy of individual laser pulses, as they are only little scattered. Further, the number of returned pulses is reduced. A smoother surface reflects the laser pulses more directed, reducing the probability of receiving a reflected laser pulse.

4.2 On hypothesis 2: Wakes and increased turbulence

4.2.1 Turbulence in the wake

The reduction of the wind speed by wind turbines leads to an area of low wind speed which can generate large horizontal shear at the boundary between the undisturbed wind field and the wake. For flights perpendicular to the wake at hub height, the measurements show strongly enhanced turbulence parameters at the edges of the wakes. For pronounced far-reaching wakes, the turbulent kinetic energy (TKE) at the edges od the wake is still at the same level several 10 km behind the wind park (Figure 10b). During the airborne measurements, the enhanced aircraft vibrations during entering and leaving the wake were noticeable to the crew. Turbulence was found to be particularly enhanced for high wind speed gradients between the wake and the undisturbed flow
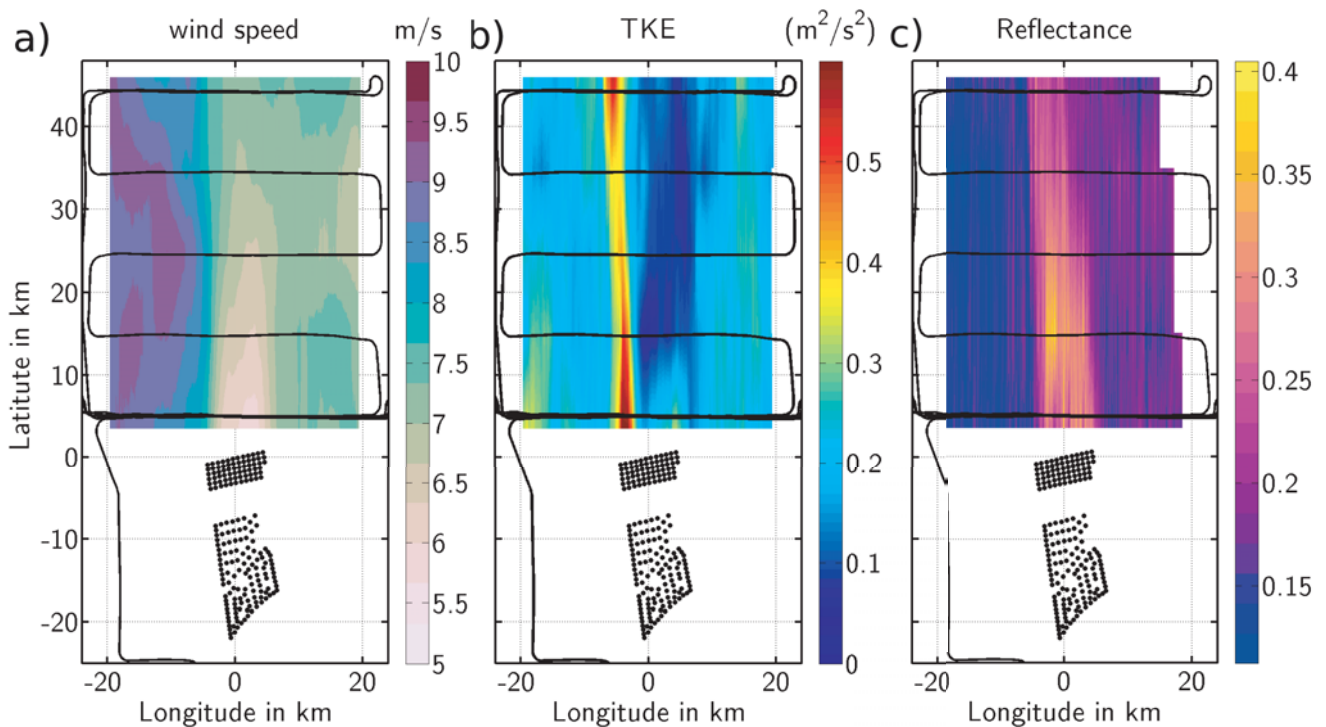
366   A. Platis et al.: Results of the project WIPAFF   *Meteorol. Z. (Contrib. Atm. Sci.)*

29, 2020

Figure 10: Measurements of wind speed (a), turbulent kinetic energy (b) and surface reflectance (c) downwind of the wind parks Amrumbank West, Nordsee Ost and Meerwind Süd/Ost. The measurement flight took place on 10 September 2016. Adapted from PLATIS et al. (2018).

(Figure 10a, b), and for denser wind park geometries. In contrast, within the wake, turbulent kinetic energy is reduced even compared to the undisturbed flow (Figure 10b).

As any change in wind field at the turbine level affects also the sea surface, SAR is capable of detecting the horizontal shear on the edge of the wake through the roughness as well. Figure 9a shows an example of the roughness by the indication of the Normalized Radar Cross Section (NRCS), obtained by Sentinel-1A on June 18, 2017 at 05:48 UTC during stable conditions (air temperature at 50 m was 16 °C and 15.4 °C for the sea surface temperature). Strong increases of NRCS and friction velocity can be seen at the boundaries of wakes downstream wind parks at the northern edge of the two wind parks.

Similarly, the derived wind speed at 10 m altitude (Figure 9b) using the geophysical model function CMOD5N GMF (HERSBACH et al., 2007; VERHOEF et al., 2008) tuned for C-band displays an increase of amplitude at the edge. These features can be explained by the considerable horizontal shear that exists between the wind field inside the wake and outside the wake. This shear leads to an increase in turbulence, which is also captured in numerical model simulations (ABKAR and PORTÉ-AGEL, 2015a). The higher turbulence levels at the boundaries of wakes have also been confirmed by airborne lidar surface roughness measurements (PLATIS et al., 2018), see Figure 10. This turbulence then causes an increase in the downward momentum flux, which can

explain a growth of the friction velocity and hence the radar cross section. This effect can be expected to be particularly effective in stable situations with strong vertical wind speed gradients. These are actually the conditions where wakes are most visible on SAR images. A semi-empirical model to describe the effect of increased downward momentum flux associated with turbulence on surface roughness measured by SAR is given in DJATH et al. (2018).

4.2.2 TKE above the wind park

The mixing above offshore wind parks determines the wake recovery as pointed out in EMEIS (2010). Consequently, mesoscale WPPs should represent the enhanced mixing above offshore wind parks to capture the correct wake extent. In SIEDERSLEBEN et al. (2020) we presented three aircraft case studies, where the TKE above the wind parks Godewind and neighbouring wind parks Nordsee Ost and Meerwind Süd/Ost was measured and compared to mesoscale simulations.

The most important ingredient for capturing the TKE above offshore wind parks with WPPs are correctly simulated upwind conditions. The WPP of FITCH et al. (2012) captured the enhanced TKE above the wind parks Godewind 1, 2 during onshore winds. In contrast, the model overstimated the TKE above the wind parks during offshore winds. By the use of vertical profiles taken by the aircraft close to the coast, we showed that the boundary layer parameterization (MYNN 2.5, NAKANISHI and NIINO, 2004) was not able to represent the

transition from land to open ocean close to the coast in case of offshore winds. Hence, we suggest the deviation of the simulated and observed TKE above offshore wind parks is largely rooted in the deviation of the simulated and observed upwind conditions. These results agree with the findings in SIEDERSLEBEN et al. (2018a) (Section 4.1.4) where the overestimated extent of the wake was related to deviations between the simulated and observed stratification of the atmosphere.

We recommend using the TKE source of the WPP of FITCH et al. (2012) for offshore wind park simulations during stable conditions, especially for simulations having a horizontal grid coarser or equal to 5 km. For example, simulations with a horizontal grid size of 16 km did not capture the enhanced mixing over the wind parks although the WPP of FITCH et al. (2012) adds additonal TKE to the model to account for the not resolved shear within the simulations.

The WPP of FITCH et al. (2012) adds too much TKE at the upwind side of a wind park. During two case studies it was observed that TKE above the wind parks increased with the path of the air through the wind park resulting in a higher TKE at the downwind side of a wind park than on the upwind side. In contrast, the WPP simulated the highest TKE at the upwind side of the wind park associated with the highest wind speeds and wind park density at the front row turbines. On the other hand, the wind speed deficit is underestimated with a disabled TKE source. Therefore, we suggest to use the TKE source for stable conditions (SIEDERSLEBEN et al., 2020) although the TKE at the upwind side of the wind park might be overestimated.

4.2.3 Wave-number spectrum vs. stability

Wave-number spectra were computed from the 10 m-wind speed derived from the SAR dataset taking into account the stability conditions based on the thermal stratification from the FINO1 data. The spectral analysis is performed for the period September 2016 to May 2017 and considered stable and unstable stratification cases. The results for all stability cases are shown in Figure 11. Each spectrum represents the average over the considered period. Although their spectral forms appear to be different at high wavenumber, the shapes look quite similar in general at low wavenumber. The slope is quite close to the $k^{-5/3}$ power law (POND et al., 1966; KAIMAL et al., 1972; NICHOLLS and READINGS, 1981; CHIN et al., 1998; WIKLE et al., 1999; CHO et al., 1999b; CHO et al., 1999a; HÖGSTRÖM et al., 2002; TULLOCH and SMITH, 2009; XU et al., 2011).

The change in stability does not affect the spectral slope in general, but rather modifies the amplitude of spectral power. The spectral power for unstable conditions (green curve in Figure 11) is indeed higher than the spectral power of stable conditions (black in Figure 11). This analysis is in agreement with the previous works (KAIMAL et al., 1972; NICHOLLS and READINGS, 1981; DJATH and SCHULZ-STELLENFLETH, 2020).
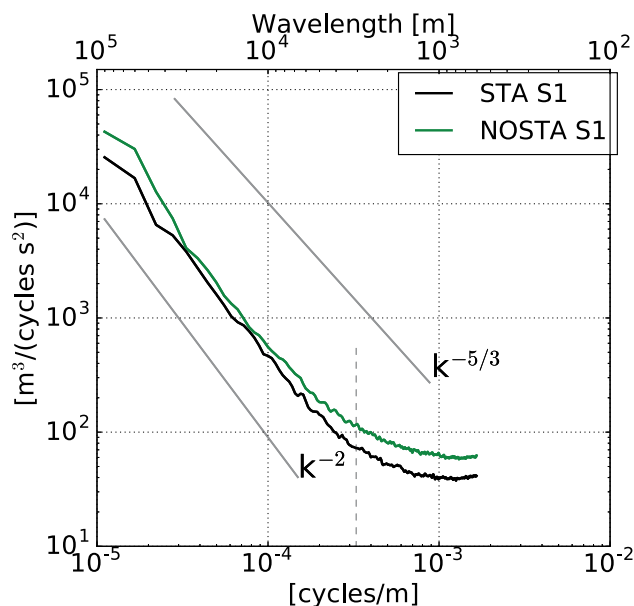

Figure 11: Wavenumber spectra computed from near-surface wind fields derived from Copernicus Sentinel-1 data. "STA" stands for stable cases (black curve) and "NOSTA" for unstable cases (green curve).

The high spectral power associated with the unstable stratification confirms that the unstable flows are more turbulent than stable flows. Within the wind park wake context, the generation of turbulence increases mixing and therefore dampens the wake, which lead to having no or short wakes during unstable conditions, while long wakes are pronounced for stable stratification (CHRISTIANSEN and HASAGER, 2005; DJATH et al., 2018).

4.2.4 Anisotropy spectra aligned wind direction

2D wind spectra were also computed from the mean normalised wind speed (Figure 12). As the stable atmospheric boundary layers are favorable conditions, where wakes are most pronounced, the spectrum is estimated by averaging over the spectra of SAR derived wind fields for stable cases as derived from FINO1. The spectrum is oriented with the wind direction along the horizontal axis. It is interesting to note, that the isolines are bunched in the wind direction, at least for wave lengths shorter than about 10 km. This is equivalent to the occurrence of wind field structures, which are aligned in wind direction. For instance, the atmospheric boundary rolls are aligned with wind direction and are used to estimate the wind direction on SAR images (KOCH, 2004).

4.3 On hypothesis 3: Impact on other wind parks downstream

The impact of far wakes on the environment and on other wind parks depends on the wake length and on the shape of the wind speed recovery within the wakes. In CAÑADILLAS et al. (2020) data from 11 flight measurements collected within the wakes at several downstream
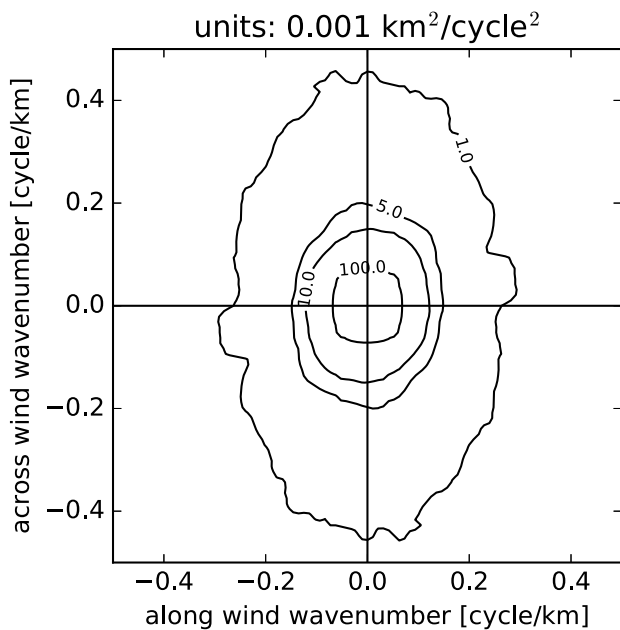
Figure 12: Mean 2D wind modulation spectrum estimated from SAR derived normalised wind field spectra.

distances of two offshore wind park clusters were analyzed.

A method was developed to extract the wake recovery function of each measurement flight and a median value was computed for each stable and neutral/unstable atmospheric conditions group. It allowed to calibrate the engineering model WindFarmer used in WIPAFF project. For further details please refer to Cañadillas et al. (2020).

The findings from this study support the results in Section 4.1.1–4.1.2 that stable stratifications is associated with significantly longer wakes characterized by a slower wind speed recovery compared to unstable conditions. The results show that the average wake length under stable conditions exceeds 50 km, while under neutral/unstable conditions, the wake length typically extends to 15 km similar to the results presented in Section 4.1.2. The default settings of the engineering model WindFarmer have to be modified to account for a slower wind speed recovery in stable stratification, as the observed length of wakes under these conditions highly exceeds the wake length arising from the default settings (see Figure 7).

The examination of the effect of the modified recovery on the park efficiency of an isolated downstream wind farm cluster reveals that, for distances > 30 km, the calculated reduction of the wind park efficiency does not exceed 0.5 %. This is considered to be a lower limit of the actual economic effect, as distances between most wind park clusters in the German exclusive economic zone (EEZ) and other offshore regions are < 30 km. However, modelling wakes at distances < 30 km downstream requires modification of not only the stability behaviour of the wind speed recovery, but also of the direct wake and IBL models.

4.3.1 Influence of park architecture

The effect of wind park architecture was estimated when distinct wakes were visible downstream of single wind parks within the same atmospheric conditions. As presented in Platis et al., in review this was the case for the Flights 25, 30 and 31 within the WIPAFF project. Here, a distinct example is shown in Figure 4 for the case study Flight 31. The wakes of the two adjacent parks Meerwind Süd/Ost (MSO) and Nordsee Ost (NO) are similar in their length (15 to 21 km). However, they differ in the initial wind speed deficit, i.e. 29 % for MSO and 19 % for NO. The wake of the very dense wind park AW is significantly longer at 38 km with initial wind deficit of 28 %. Other case studies showed similar observations in Platis et al., in review. As a consequence, it can be concluded that a clear influence of the park layout is evident and longer wakes appeared with a denser alignment of wind turbines in contrast to a low-density wind park. Therefore, to minimize the impact of downstream installations a less narrow alignment of the wind turbines could be considered in future offshore wind park planning.

4.4 On hypothesis 4: Impact of wind-park wakes on local climate and surface fluxes

Given the warming and cooling in the rotor layer associated with the enhanced vertical mixing at the rotor area (Section 4.1.3) the question arises whether wind parks can alter local climate.

A change in local climate would be equal to a change in the energy budget of the atmosphere. According to Trenberth et al. (2001) and Porter et al. (2011) a change in the energy budget of the atmosphere is associated with a change in radiation budget and/or in the turbulent surface fluxes. Hence, it is relevant whether the temperature and moisture changes at hub height as investigated in Siedersleben et al. (2018b) are associated with temperature and moisture changes at the surface that in turn could enhance the turbulent fluxes at the surface resulting in a change of the energy budget of the atmosphere. Temperature and moisture changes were well observed on 10 September 2016, hence, we investigated the potential impact of all planned and existing offshore wind parks in the German Bight on the turbulent surface fluxes (i.e. sensible and latent heat flux) by the use of WRF simulations. The locations of the planned wind parks follow plans of the Bundesamts für Seeschifffahrt und Hydrographie (BSH) published in 2015 (Figure 13). Although such a numerical simulation can not give a answer on whether offshore wind farms have an impact on the local climate or not, we can still determine the maximal impact of offshore wind farms on the boundary layer by simulating a day, that was characterised by large wakes in the German Bight. Based on these results further studies should be conducted, investigating the impact of offshore wind farms on the local climate.
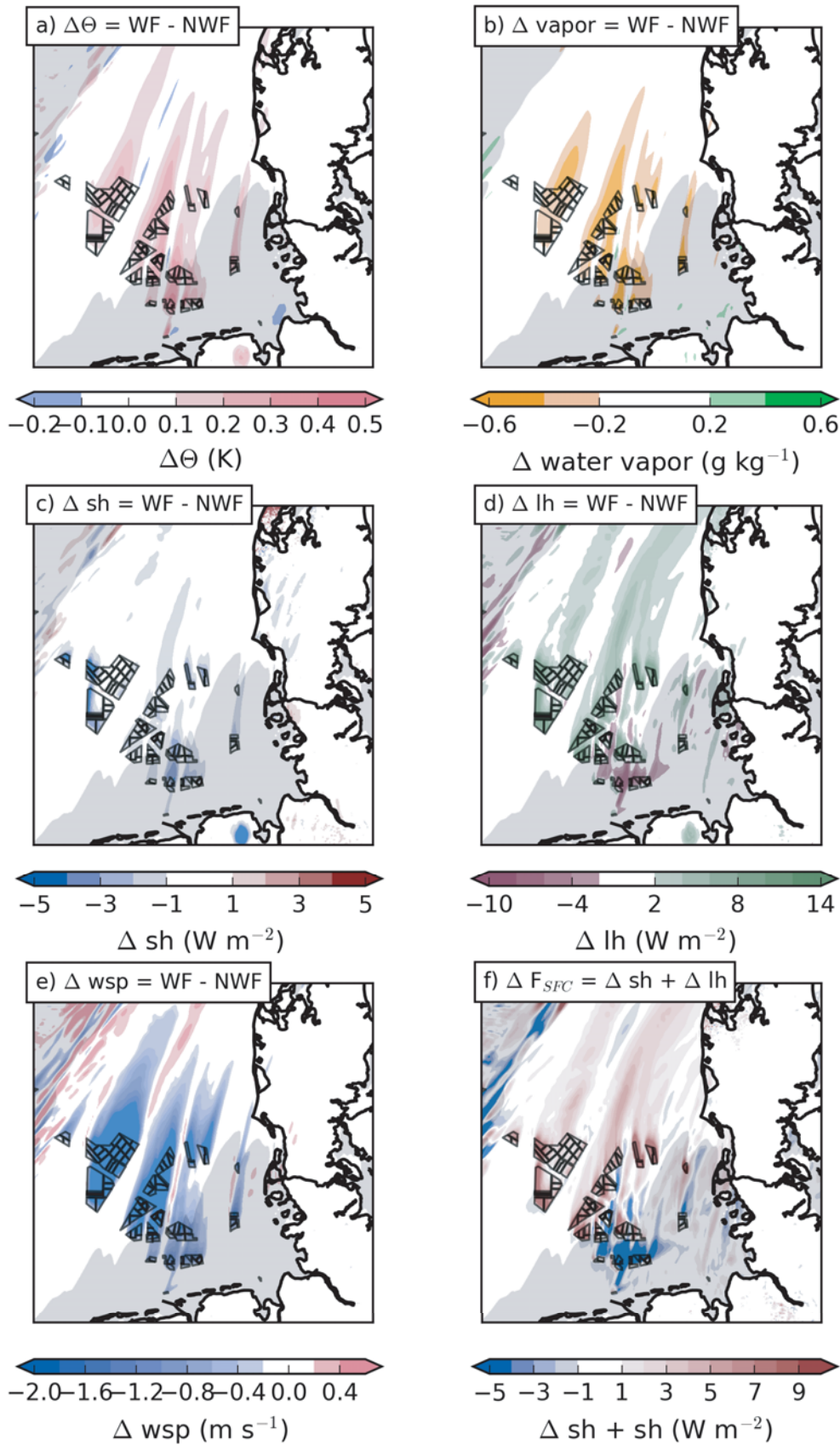
Figure 13: The impact of all potentially planned offshore wind parks at the North Sea for the meteorological situation 10 September 2016 averaged from 08:00 UTC to 09:00 UTC. Shown is the difference at hub height of (a) potential temperature, (b) water vapor mixing ratio and (e) wind speed between a simulation with wind parks (WF) and a simulation with no wind parks (NWF). The resulting changes of sensible heat flux (sh) and latent heat flux (lh) are shown in (c) and (d). The sum of differences in sensible and latent heat flux is shown in (f). The gray shading depicts areas where the SST is higher than the air temperature. Taken from SIEDERSLEBEN (2019).

Although some wind parks in the simulations are much bigger than already existing wind parks in the German Bight, the impact on temperature and water vapor at hub height is not larger than observed on 10 September 2016 (Figure 13a–b). For example, the simulations suggest a warming and a drying at hub height in the order of 0.5 K and 0.5 g kg^{-1} downwind of the large offshore wind park cluster located in the west of the domain. For comparison, the already existing wind parks around Amrumbank West cause a similar warming signal at hub height.

The warming induced by the wind parks in the rotor area is partly associated with a decreased sensible heat flux at the surface (Figure 13c). Two different processes drive the reduction of the sensible heat flux rooted in the different temperature gradients between the SST and the lowest model level located at 17 m AMSL (Figure 14). On 10 September 2016 we encountered areas with a lower air temperature than SST (i.e. gray shaded area in Figure 13, SIEDERSLEBEN, 2019). During non-waked conditions the sensible heat flux is orientated towards the atmosphere in these regions, resulting in a warming of the lower atmosphere (Figure 14a). According to aircraft measurements recorded on 10 September 2016, the warming induced by the wind turbines was also effective at 60 m AMSL (see Figure 4a in SIEDERSLEBEN et al., 2018b). The simulations indicate that the warming at the rotor area even spread down to the ocean's surface. Consequently, a higher surface temperature results in a reduction of the temperature gradient between air temperature and SST that in turn weakens the sensible heat flux towards the atmosphere as it is schematically sketched in Figure 14a). In contrast, the sensible heat flux is orientated towards the ocean in case of a lower SST than air temperature (*not* gray shaded area in Figure 13) during non-waked conditions. However, a warming at the ocean's surface results in an increased temperature gradient between air temperature and SST, resulting in an larger sensible heat flux pointing towards the ocean (Figure 14b). Therefore, the net effect of the warming at the surface is an increased sensible heat flux towards the ocean (Figure 14b). However, the changes in the sensible heat flux are not larger than 3 W m^{-2}.

The impact of offshore wind parks on the latent heat flux is determined by the temperature gradient between SST and the temperature at the lowest model level (Figure 13d). In areas with a higher SST than air temperature the simulated latent heat flux is decreased. In contrast, the latent heat flux is increased in areas with a higher air temperature than SST. As humidity usually has a strong vertical gradient in the marine boundary layer (decreasing with height), the latent heat flux is pointing upward regardless of the temperature gradient. Obviously, the dryer air within the wakes of larger offshore wind parks enhances the vertical moisture gradient, that in turn should enhance the latent heat flux towards the atmosphere. However, this is only true for areas with a higher air temperature than SST (Figure 13d). In contrast, in regions with a lower SST than air temperature,
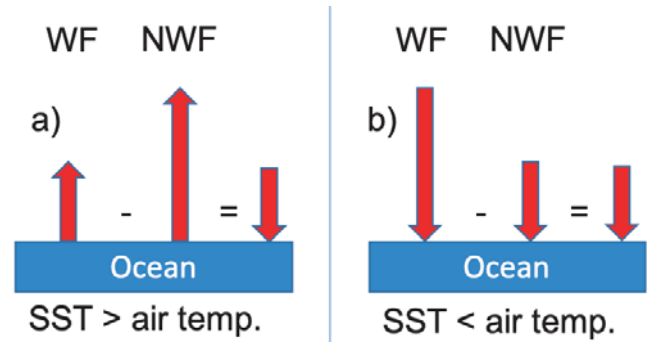

Figure 14: Schematic sketch of impact of offshore wind parks on the sensible heat flux in case of (a) a SST higher than the air temperature and (b) vice versa. WF is a wind park simulation with the wind farm parameterization turned on, while NWF has the parameterization switched off. Taken from SIEDERSLEBEN (2019).

we observe a decreased latent heat flux (purple contours in Figure 13e), although the latent heat flux is supposed to increased due to dryer air within the wake. Hence, we suggest, that the weakening of the temperature gradient between SST and air temperature mainly drives the changes in the latent heat flux.

The overall change in the surface fluxes is driven by the changes in the latent heat flux (Figure 13f), in case of inversions close to the rotor height. As the impact on 10 September 2016 on the latent heat flux is almost twice as much than the changes in the sensible heat flux the net impact on the surface fluxes is dominated by the changes in latent heat flux. As the changes in the latent heat flux are determined by the temperature gradient between the lowest model level and SST, so is the overall impact: A cooling effect is present in areas with a higher air temperature than SST and vice versa. However, we only observed a change in the latent heat flux associated with the existence of an inversion close to rotor height SIEDERSLEBEN et al., 2018b. Hence, the latent heat flux only dominates the overall impact in case of an inversion close to the rotor area otherwise only the sensible heat flux is affected.

The effects discussed above were observed in six of our flights, nevertheless for a sound climatology reliable conclusion, further studies are mandatory.

5   Conclusion/Outlook

A unique dataset from airborne *in situ* data, remote sensing by laser scanner and SAR gained during the WIPAFF project proves that wakes up to several tens of kilometers exist downstream of offshore wind farms. The wind speed deficits in the wakes and their length tend to be larger in stable than in unstable conditions. The results show that the average wake lengths under stable conditions exceed 50 km, while under neutral/unstable conditions, the wake length amounts to 15 km or less. Data also indicates that a denser wind park layout increases the wake length additionally due

to a higher initial wind speed deficit. Turbulence occurs at the edges of the wakes due to shear between the reduced wind speed inside the wake and the undisturbed flow. The intensity depends on the strength of the wind speed gradient and is further enhanced for denser wind park geometries. In contrast, within the wake, turbulent kinetic energy is reduced even compared to the undisturbed flow.

The observational data of the WIPAFF project was further compared to industrial, analytical and mesoscale models. The respective models show in general a good correlation with the measured wake lengths, nevertheless, they also show deficiencies:

- As a first order approximation the analytical model seems to work well, however it has to be optimized to be able to account for the park layout and turbine turbine-induced turbulence left over from the wind park. This has to be improved in the future.
- The engineering model WindFarmer underestimates the wake length during stable conditions when using the default settings. Therefore, default settings of the engineering model WindFarmer have been modified to account for a slower wind speed recovery in stable stratification (CAÑADILLAS et al., 2020).
- The mesoscale WRF model enables the simulation of a complete area like the German Bight. However, the results of the simulations show that the WRF model is highly sensitive to the upwind conditions. During offshore winds (advecting warm air over the ocean) strong inversions developed at rotor height that are challenging for a mesoscale model. Hence, the upstream wind speed was sometimes underestimated due to a wrongly predicted stratification in the model.

To accomplish accurate predictions of the wind energy production by numerical models, further effects have to be taken into account, e.g. the blockage effects of wind parks or how the state of the operation of wind parks influences the wakes, which requires the analysis of operational data. As such data was not available in the WIPAFF project, this is a topic of future research and implementation in numerical models.

Besides the wake effects, the influence of offshore wind parks on the marine bounadry layer was investigated by using the airborne observations and the WRF model. The impact on the marine boundary layer depends on several parameters. First of all, wind parks can cause a warming or a cooling at hub height during stable conditions as discussed in Section 4.1.3. However, the inversion can also be located such that a cooling at the ocean's surface takes place, although we only presented here a warming case. Secondly, only in case of a pronounced inversion close to hub height we simulated and observed a change in the water vapor mixng ratio corresponding to changes in latent heat flux. Thirdly, the net impact on the latent heat flux was determined by the temperature gradient between SST and the ambient air temperature.

Several potential impacts of offshore wind parks on the marine boundary layer were not discussed in this study i.e the formation of clouds. HUANG and HALL (2015) and BOETTCHER et al. (2015) showed that large offshore wind park could have an influence on the cloud cover. Consequently, wind parks could have an influence on the radiation budget as well. These aspects were not presented as we could not identify a clear impact of offshore wind parks on the cloud cover or any radiation budget due to lacking equipment.

Given the high sensitivity of the simulated impacts of offshore wind farms, studies making general statements about the impacts of offshore wind farms based on numerical climate or mesoscale models should be carefully examined. As discussed above, simulated impact on the local climate is extremely sensible to the simulated stability in the lowest 200 m of the marine boundary layer. Within the WIPAFF project we showed that mesoscale simulations were lacking to represent the stable boundary layer during offshore winds close to the coast, although most wind parks are in the transition area from coast to open sea and their impact is largest during stable conditions (SIEDERSLEBEN et al., 2018b).

The above documented results may have several consequences.

5.1 Wind direction-based layout of wind parks

Analysis of data from FINO1 for the year 2005 shows a clear correlation between wind direction and atmospheric stratification in the North Sea (EMEIS et al., 2016). Stable situations are coupled to the main wind direction (South-West). This direction-stability correlation is assumed to be typical for the two temperate latitude west-wind belts on both hemispheres of the globe, because it is caused by the usual sequence of warm sector winds having a poleward component followed by cold sector winds having an equatorward component in eastward moving low-pressure systems. The WIPAFF results clearly documented the dependence of the wake intensity and wake length on atmospheric stratification. Therefore, it could be advisable that wind park layout and park cluster layout take this dependence into account. Figure 15 shows a possible array of wind parks in the German Bight which reflects this correlation. Distances between single turbines within wind parks and between entire parks are larger along the most frequent direction of stably stratified flow (from Southwest to Northeast) and they are shorter along the perpendicular direction of unstably stratified flow.

5.2 Additional measurement requirements and stability measures for the marine BL

For future estimations of wind park power output and for improving analyses of offshore wind park wakes, a crucial parameter was found to be profiles of temperature and the stability parameter. Temperature inversions occur at different altitudes above, below and within the rotor area. A near-surface, predominantly convective layer
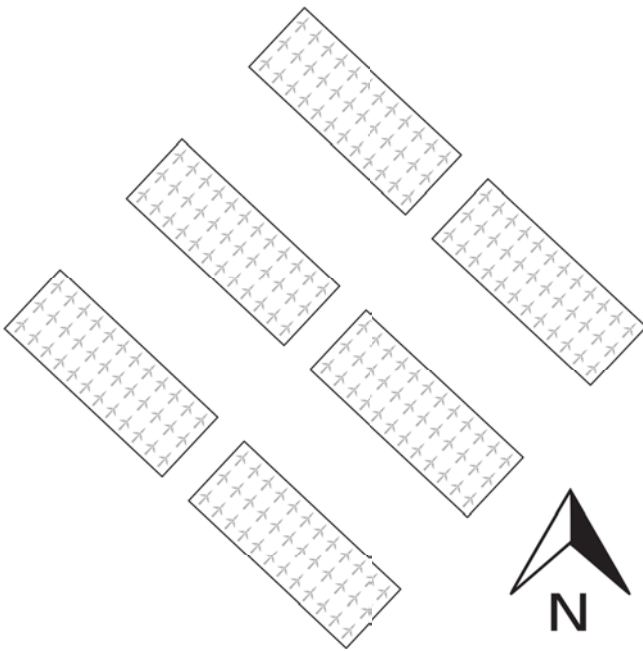
Figure 15: Schematic of stability-dependent wind park layout in the German Bight. Crosses denote single wind turbines and boxes indicate wind parks. North is towards the top. (Adapted from Emeis et al., 2016)

may be present and an inversion with more stable conditions may be found aloft. Therefore, a simple approach for defining stability, e.g. the temperature difference between the sea surface and the atmosphere at one particular altitude, is not suitable for describing stability conditions and wake development. In addition, other stability parameters are partly inconsistent with each other. Therefore, defining stability measures for the marine boundary layers which can be representative for atmospheric stability for an offshore wind park and the evolution of wind park wakes is a very crucial task for the future.

Moreover, the representation of temperature profiles in numerical simulations and the deduced stability need higher accuracy and improvement. The comparison of the airborne observations and WRF simulations show potential for improving the representation of coastal effects, where temperature profiles develop from the coast to the wind parks. For example, from the simulations of 15 October 2017 two profiles are compared to the simulations, one close to the coast, one further offshore (Figure 16). Close to the coast the simulation and observation show an inversion. However, the inversion of the simulation is located above the rotor area, whereby the inversion in the observations is located within the rotor area. Further offshore, the performance of the model improves slightly. Nevertheless, the height of the inversion is still overestimated by 150 m. The numerical simulations where performed with the setup as described in Siedersleben et al. (2018a). As the development of the stability for the flow above the coast strongly influences the wake extent, an improvement of the simulations is

required for correctly representing the inflow conditions reaching the wind park. The availability of additional measurements of temperature profiles at a coastal and at an offshore locations could serve as reference and would contribute to a better understanding of the processes in the atmospheric boundary layer and the interaction with wind parks and lead to improvement of numerical simulations.

5.3   Impact on cloud development

On three out of 41 measurement flights, the formation of small patches of clouds directly above the wind park was observed. The cloud patches were transported downwind. No such clouds were observed in the lee and next to the wind park. Cloud formation was observed on days with relative humidity close to saturation, and slightly stable conditions. The documentation of the clouds was attempted by photographing. However, the image quality was hampered by other cloud layers above. The sensors on board were not suitable for systematic analyses of the phenomenon and its importance. This should be addressed in future research in combination with the analysis of downward heat and humidity fluxes above wind parks.

5.4   Future SAR data evaluation

About one third of the SAR scenes with visible wake structures show increased radar cross section values for roughly the first 10 km of the wake downstream the wind park. There are several approaches to explain this phenomenon, which seems to be a paradox at first sight. One possible explanation proposed in Djath et al. (2018) is based on the hypothesis of increased downward momentum fluxes caused by turbulence introduced by the wind turbines. Making this assumption, SAR data would provide very valuable information on the advection and dissipation of turbulence in the vicinity of offshore wind parks. However, observational evidence is missing to confirm or refute this or a number of other possible mechanisms to explain the effect. Measurements are a challenge in this context, because the sea surface roughness measured by the radar is strongly dependent on the detailed structured of the atmospheric boundary layer close to the water. New measurement technologies and sampling approaches are currently investigated to obtain more information on this important region. These activities are not only of high value to improve our understanding of the atmospheric processes around offshore wind parks, but are of more general relevance in the context of atmosphere/ocean interaction, which is a field of intense research worldwide.

A topic that is directly related to the phenomenon just described, is the derivation of wind speed information above the sea surface from microwave radar data. Radar measurements have a direct physical connection to the friction velocity at the surface, but wind speeds at higher levels depend on the stability conditions in
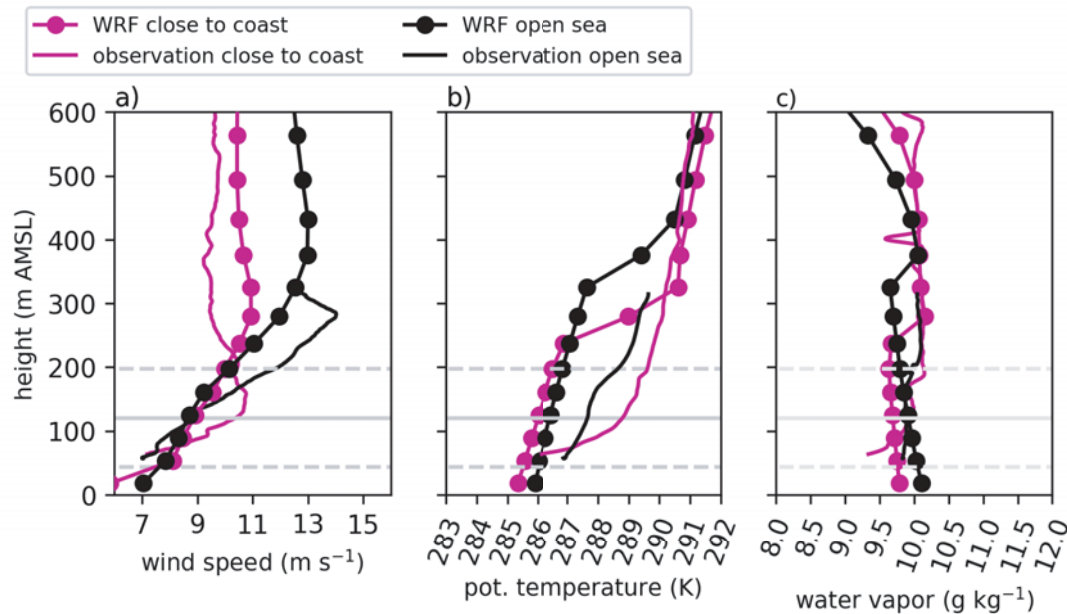
Figure 16: Vertical profiles of wind speed (a), potential temperature (b) and water vapour mixing ratio (c) obtained by probing the atmosphere with the research aircraft on 15 October 2017 close to the coast (magenta solid lines) and further offshore (black solid lines). The corresponding locations of the vertical profiles are shown in detail in Figure 1. The interpolated WRF data along the climb flights is shown with the solid lines having the circles on top, whereby each circle represents a vertical level of the simulation.

the boundary layer, which are usually not well known. The empirical functions used for SAR wind speed retrieval so far were usually derived based on observation data sets taken in the open ocean, making very simplifying assumptions about the conditions in the atmosphere. This is another area of research, where more sophisticated measurements of the atmospheric boundary layer in near coastal areas could help to optimise the exploitation of SAR information for offshore wind park applications. This issue is also related to the more general question about the optimal integration of satellite, *in situ* and model data to provide efficient information products to the offshore wind park community.

Acknowledgments

References

Abkar, M., F. Porté-Agel, 2015a: Influence of atmospheric stability on wind-turbine wakes: A large-eddy simulation study. – Phys. Fluids **27**, 035104.

Abkar, M., F. Porté-Agel, 2015b: A new wind-farm parameterization for large-scale atmospheric models. – J. Renew. Sustain. Energy **7**, 013121.

Ainslie, J., 1988: Calculating the flow field in the wake of wind turbines. – J. Wind Engin. Indust. Aerodyn. **27**, 213–224, DOI: 10.1016/0167-6105(88)90037-2.

Armstrong, A., R.R. Burton, S.E. Lee, S. Mobbs, N. Ostle, V. Smith, S. Waldron, J. Whitaker, 2016: Ground-level climate at a peatland wind farm in Scotland is affected by wind turbine operation. – Env. Res. Lett. **11**, 044024.

Bärfuss, K., R. Hankers, M. Bitter, T. Feuerle, H. Schulz, T. Rausch, A. Platis, J. Bange, A. Lampert, 2019: In-situ airborne measurements of atmospheric and sea surface parameters related to offshore wind parks in the German Bight. – PANGAEA, published online. DOI: 10.1594/PANGAEA.902845.

Barthelmie, R., S. Frandsen, P. Rethore, L. Jensen, 2007: Analysis of atmospheric impacts on the development of wind turbine wakes at the Nysted wind farm. – In: European Offshore Wind Conference, volume **6**.

Barthelmie, R.J., L. Jensen, 2010: Evaluation of wind farm efficiency and wind turbine wakes at the Nysted offshore wind farm. – Wind Energy **13**, 573–586.

Barthelmie, R.J., K. Hansen, S.T. Frandsen, O. Rathmann, J. Schepers, W. Schlez, J. Phillips, K. Rados, A. Zervos, E. Politis, others, 2009: Modelling and measuring flow and wind turbine wakes in large wind farms offshore. – Wind Energy **12**, 431–444.

Blahak, U., B. Goretzki, J. Meis, 2010: A simple parameterization of drag forces induced by large wind farms for numerical weather prediction models. – In: Proceedings of the European Wind Energy Conference & Exhibition.

Bodini, N., D. Zardi, J.K. Lundquist, 2017: Three-dimensional structure of wind turbine wakes as measured by scanning lidar. – Atmos. Measur. Techn. **10**, 2881–2896.

BOETTCHER, M., P. HOFFMANN, H.J. LENHART, H. SCHLÜNZEN, R. SCHOETTER, 2015: Influence of large offshore wind farms on north german climate. – Meteorol. Z. **24**, 465–480.

BOSSANYI, E., G. WHITTLE, P. DUNN, N. LIPMAN, P. MUSGROVE, C. MACLEAN, 1980: The efficiency of wind turbine clusters. – In: 3rd International symposium on wind energy systems, 401–416.

CAÑADILLAS, B., R. FOREMAN, V. BARTH, A. PLATIS, S.K. SIEDERSLEBEN, J. BANGE, A. LAMPERT, K. BÄRFUSS, R. HANKERS, J. SCHULZ-STELLENFLETH, B. DJATH, S. EMEIS, T. NEUMANN, 2020: Offshore wind farm wake recovery: Airborne measurements and its representation in engineering models. – Wind Energy, published online. DOI: 10.1002/we.2484.

CHAMORRO, L.P., F. PORTE-AGEL, 2011: Turbulent flow inside and above a wind farm: a wind-tunnel study. – Energies **4**, 1916–1936.

CHIN, T.M., R.F. MILLIFF, W.G. LARGE, 1998: Basin-scale, high-wavenumber sea surface wind fields from a multiresolution analysis of scatterometer data. – J. Atmos. Oceanic Technol. **15**, 741–763.

CHO, J.Y., R.E. NEWELL, J.D. BARRICK, 1999a: Horizontal wavenumber spectra of winds, temperature, and trace gases during the pacific exploratory missions: 2. gravity waves, quasi-two-dimensional turbulence, and vortical modes. – J. Geophys. Res. **104**, 16297–16308.

CHO, J.Y.N., Y. ZHU, R.E. NEWELL, B.E. ANDERSON, J.D. BARRICK, G.L. GREGORY, G.W. SACHSE, M.A. CARROLL, G.M. ALBERCOOK, 1999b: Horizontal wavenumber spectra of winds, temperature, and trace gases during the Pacific Exploratory Missions: 1. Climatology. – J. Geophys. Res. Atmos. **104**, 5697–5716.

CHRISTIANSEN, M.B., C.B. HASAGER, 2005: Wake effects of large offshore wind farms identified from satellite SAR. – Remote Sens. Env. **98**, 251–268.

CORSMEIER, U., R. HANKERS, A. WIESER, 2001: Airborne turbulence measurements in the lower troposphere onboard the research aircraft dornier 128-6, D-IBUF. – Meteorol. Z. **10**, 315–329.

DJATH, B., J. SCHULZ-STELLENFLETH, 2020: Wind speed deficits downstream offshore wind parks – a new automised estimation technique based on satellite synthetic aperture radar data. – Meteorol. Z. **28**, 499–515. DOI: 10.1127/metz/2019/0992.

DJATH, B., J. SCHULZ-STELLENFLETH, B. CAÑADILLAS, 2018: Impact of atmospheric stability on X-band and C-band synthetic aperture radar imagery of offshore windpark wakes. – J. Renew. Sustain. Energy **10**, 043301.

DNV-GL, 2013a: WindFarmer v.5.2 theory manual. – Technical report, Garrad Hassan and Partners, Ltd.

DNV-GL, 2013b: WindFarmer v.5.2 validation report. – Technical report, Garrad Hassan and Partners, Ltd.

DÖRENKÄMPER, M., B. WITHA, G. STEINFELD, D. HEINEMANN, M. KÜHN, 2015a: The impact of stable atmospheric boundary layers on wind-turbine wakes within offshore wind farms. – J. Wind Engineer. Indust. Aerodyn. **144**, 146–153.

DÖRENKÄMPER, M., M. OPTIS, A. MONAHAN, G. STEINFELD, 2015b: On the offshore advection of boundary-layer structures and the influence on offshore wind conditions. – Bound.-Layer Meteor. **155**, 459–482.

EMEIS, S., 2010: A simple analytical wind park model considering atmospheric stability. – Wind Energy **13**, 459–469.

EMEIS, S., 2018: Wind energy meteorology: atmospheric physics for wind power generation. – Springer, 255 + XXVI pp.

EMEIS, S., S. FRANDSEN, 1993: Reduction of horizontal wind speed in a boundary layer with obstacles. – Bound.-Layer Meteorol. **64**, 297–305.

EMEIS, S., S. SIEDERSLEBEN, A. LAMPERT, A. PLATIS, J. BANGE, B. DJATH, J. SCHULZ-STELLENFLETH, T. NEUMANN, 2016: Exploring the wakes of large offshore wind farms. – J. Phys. Conference Series **753**, 092014.

FIEDLER, B., A. ADAMS, 2014: A subgrid parameterization for wind turbines in weather prediction models with an application to wind resource limits. – Adv. Meteor. **2014**, 696202. DOI: 10.1155/2014/696202.

FITCH, A.C., J.B. OLSON, J.K. LUNDQUIST, J. DUDHIA, A.K. GUPTA, J. MICHALAKES, I. BARSTAD, 2012: Local and mesoscale impacts of wind farms as parameterized in a mesoscale NWP model. – Mon. Wea. Rev. **140**, 3017–3038.

FOREMAN, R., B. CAÑADILLAS, T. NEUMANN, S. EMEIS, 2017: Measurements of heat and humidity fluxes in the wake of offshore wind turbines. – J. Renew. Sustain. Energy **9**, 053304.

FRANDSEN, S., 1992: On the wind speed reduction in the center of large clusters of wind turbines. – J. Wind Engin. Indust. Aerodyn. **39**, 251–265.

FRANDSEN, S., R. BARTHELMIE, S. PRYOR, O. RATHMANN, S. LARSEN, J. HØJSTRUP, M. THØGERSEN, 2006: Analytical modelling of wind speed deficit in large offshore wind farms. – Wind Energy **9**, 39–53.

HANSEN, K.S., R.J. BARTHELMIE, L.E. JENSEN, A. SOMMER, 2012: The impact of turbulence intensity and atmospheric stability on power deficits due to wind turbine wakes at horns rev wind farm. – Wind Energy **15**, 183–196.

HASAGER, C., L. RASMUSSEN, A. PEÑA, L. JENSEN, P.E. RÉTHORÉ, 2013: Wind farm wake: The Horns Rev photo case. – Energies **6**, 696–716.

HASAGER, C., N. NYGAARD, P. VOLKER, I. KARAGALI, S. ANDERSEN, J. BADGER, 2017: Wind farm wake: The 2016 Horns Rev photo case. – Energies **10**, 317.

HASAGER, C.B., P. VINCENT, J. BADGER, M. BADGER, A. DI BELLA, A. PEÑA, R. HUSSON, P.J. VOLKER, 2015: Using Satellite SAR to Characterize the Wind Flow Around Offshore Wind Farms. – Energies **8**, 5413–5439, DOI: 10.3390/en8065413.

HERSBACH, H., A. STOFFELEN, S. DE HAAN, 2007: An improved C-band scatterometer ocean geophysical model function: CMOD5. – J. Geophys. Res. Oceans **112**, published online. DOI: 10.1029/2006JC003743.

HÖGSTRÖM, U., J. HUNT, A.S. SMEDMAN, 2002: Theory and measurements for turbulence spectra and variances in the atmospheric neutral surface layer. – Bound.-Layer Meteor. **103**, 101–124.

HUANG, H.Y., A. HALL, 2015: OFFSHORE WIND DEVELOPMENT IMPACTS ON MARINE ATMOSPHERIC ENVIRONMENT. – Available online at http://www.energy.ca.gov/2016publications/CEC-500-2016-023/CEC-500-2016-023.pdf.

JACOBSON, M.Z., C.L. ARCHER, 2012: Saturation wind power potential and its implications for wind energy. – Proc of the Natl Acad of Sci USA **109**, 15679–15684.

JENSEN, N.O., 1983: A note on wind generator interaction. – Risø National Laboratory Roskilde.

KAFFINE, D.T., C.M. WORLEY, 2010: The windy commons? – Env. Res. Econom. **47**, 151–172.

KAIMAL, J.C., J.C. WYNGAARD, Y. IZUMI, O.R. COTÉ, 1972: Spectral characteristics of surface-layer turbulence. – Quart. J. Roy. Meteor. Soc. **98**, 563–589.

KATIC, I., J. HØJSTRUP, N. JENSEN, 1987: A simple model for cluster efficiency. – In: W. PALZ and E. SESTO (Eds.): EWEC'86. – Proceedings. Vol. 1, 407–410.

KOCH, W., 2004: Directional Analysis of SAR images aiming at wind direction. – IEEE Transactions on Geoscience and Remote Sensing **42**, 702–710.

LAMPERT, A., K.B. BÄRFUSS, A. PLATIS, S.K. SIEDERS-LEBEN, B. DJATH, B. CAÑADILLAS, R. HANKERS, M. BIT-TER, T. FEUERLE, H. SCHULZ, T. RAUSCH, M. ANGER-MANN, A. SCHWITHAL, J. BANGE, J. SCHULZ-STELLENFLETH, T. NEUMANN, S. EMEIS, 2020: In-situ airborne measurements of atmospheric and sea surface parameters related to offshore wind parks in the German Bight. – Earth Sys. Sci. Data, **12**, 935–946.

LEE, S., M. CHURCHFIELD, P. MORIARTY, J. JONKMAN, J. MICHA-LAKES, 2012: Atmospheric and wake turbulence impacts on wind turbine fatigue loadings. – In: 50th AIAA Aerospace Sciences Meeting including the New Horizons Forum and Aerospace Exposition, 540.

LI, X., S. LEHNER, 2013a: Observation of TerraSAR-X for stud-ies on offshore wind turbine wake in near and far fields. – IEEE Journal of Selected Topics in Applied Earth Observa-tions and Remote Sensing **6**, 1757–1768.

LI, X.M., S. LEHNER, 2013b: Algorithm for sea surface wind re-trieval from terrasar-x and tandem-x data. – IEEE Transactions on Geoscience and Remote Sensing **52**, 2928–2939.

LIN, H., Q. XU, Q. ZHENG, 2008: An overview on sar measure-ments of sea surface wind. – Prog. Natural Sci. **18**, 913–919.

LISSAMAN, P., 1979: Energy effectiveness of arbitrary arrays of wind turbines. – J. Energy **3**, 323–328.

LUNDQUIST, J., K. DUVIVIER, D. KAFFINE, J. TOMASZEWSKI, 2019: Costs and consequences of wind turbine wake effects arising from uncoordinated wind energy development. – Na-ture Energy **4**, 26–34.

MARTÍNEZ-TOSSAS, L.A., M.J. CHURCHFIELD, C. MENEVEAU, 2015: Large eddy simulation of wind turbine wakes: detailed comparisons of two codes focusing on effects of numerics and subgrid modeling. – J. Phys. Conference Series **625**, 012024.

MUÑOZ-ESPARZA, D., B. CAÑADILLAS, T. NEUMANN, J. VAN BEECK, 2012: Turbulent fluxes, stability and shear in the offshore environment: Mesoscale modelling and field observations at fino1. – J. Renew. Sustain Energy **4**, 063136.

NAKANISHI, M., H. NIINO, 2004: An improved mellor–yamada level-3 model with condensation physics: Its design and veri-fication. – Bound.-layer Meteor. **112**, 1–31.

NEWMAN, B., 1977: The spacing of wind turbines in large ar-rays. – Energy conversion **16**, 169–171.

NICHOLLS, S., C.J. READINGS, 1981: Spectral characteristics of surface layer turbulence over the sea. – Quart. J. Roy. Meteor. Soc. **107**, 591–614.

NYGAARD, N.G., 2014: Wakes in very large wind farms and the effect of neighbouring wind farms. – J. Phys. Conference Series **524**, 012162.

NYGAARD, N.G., S.D. HANSEN, 2016: Wake effects between two neighbouring wind farms. – J. Phys. Conference Series **753**, 032020. DOI: 10.1088/1742-6596/753/3/032020.

PEÑA, A., O. RATHMANN, 2014: Atmospheric stability-dependent infinite wind-farm models and the wake-decay coefficient. – Wind Energy **17**, 1269–1285, DOI: 10.1002/we.1632.

PEÑA, A., O. RATHMANN, 2014: Atmospheric stability-dependent infinite wind-farm models and the wake-decay co-efficient. – Wind Energy **17**, 1269–1285.

PLATIS, A., S.K. SIEDERSLEBEN, J. BANGE, A. LAMPERT, K. BÄR-FUSS, R. HANKERS, B. CAÑADILLAS, R. FOREMAN, J. SCHULZ-STELLENFLETH, B. DJATH, OTHERS, 2018: First in situ evi-dence of wakes in the far field behind offshore wind farms. – Scientific reports **8**, 2163.

PLATIS, A., M. HUNDHAUSEN, S.K. SIEDERSLEBEN, A. LAMPERT, K. BÄRFUSS, J. SCHULZ-STELLENFLETH, B. DJATH, S. EMEIS, T. NEUMANN, B. CAÑADILLAS, J. BANGE, in review: Evalua-tion of a simple analytical model for offshore wind farm wake

recovery by in-situ data and WRF simulations. – Wind Energy, in review.

POND, S., S. SMITH, P. HAMBLIN, R. BURLING, 1966: Spectra of velocity and temperature fluctuations in the atmospheric boundary layer over the sea. – J. Atmos. Sci. **23**, 376–386.

PORTÉ-AGEL, F., Y.T. WU, C.H. CHEN, 2013: A numerical study of the effects of wind direction on turbine wakes and power losses in a large wind farm. – Energies **6**, 5297–5313.

PORTÉ-AGEL, F., H. LU, Y.T. WU, 2014: Interaction between large wind farms and the atmospheric boundary layer. – Pro-cedia Iutam **10**, 307–318.

PORTÉ-AGEL, F., M. BASTANKHAH, S. SHAMSODDIN, 2020: Wind-turbine and wind-farm flows: A review. – Bound.-Layer Meteor. **174**, 1–59.

PORTER, D.F., J.J. CASSANO, M.C. SERREZE, 2011: Analysis of the Arctic atmospheric energy budget in WRF: A com-parison with reanalyses and satellite observations. – J. Geo-physical Res. Atmos. **116**, published online. DOI: 10.1029/2011JD016622.

PROSPATHOPOULOS, J., P. CHAVIAROPOULOS, 2013: Numerical simulation of offshore wind farm clusters. – In: European Wind Energy Association, Conference proceedings.

PRYOR, S., R. BARTHELMIE, A. HAHMANN, T. SHEPHERD, P. VOLKER, 2018: Downstream effects from contemporary wind turbine deployments. – J. Phys. Conference Series **1037**, 072010. IOP Publishing.

RAJEWSKI, D.A., E.S. TAKLE, J.K. LUNDQUIST, S. ONCLEY, J.H. PRUEGER, T.W. HORST, M.E. RHODES, R. PFEIFFER, J.L. HATFIELD, K.K. SPOTH, OTHERS, 2013: Crop wind energy experiment (CWEX): observations of surface-layer, boundary layer, and mesoscale interactions with a wind farm. – Bull. Amer. Meteor. Soc. **94**, 655–672.

RAJEWSKI, D.A., E.S. TAKLE, J.K. LUNDQUIST, J.H. PRUEGER, R.L. PFEIFFER, J.L. HATFIELD, K.K. SPOTH, R.K. DOORENBOS, 2014: Changes in fluxes of heat, H2O, and CO2 caused by a large wind farm. – Agricult.l Forest Meteor. **194**, 175–187.

ROHRIG, K., V. BERKHOUT, D. CALLIES, M. DURSTEWITZ, S. FAULSTICH, B. HAHN, M. JUNG, L. PAUSCHER, A. SEIBEL, M. SHAN, OTHERS, 2019: Powering the 21st century by wind energy-options, facts, figures. – Appl. Phys. Rev. **6**, 031303.

ROY, S.B., J.J. TRAITEUR, 2010: Impacts of wind farms on sur-face air temperatures. – Proceedings of the National Academy of Sciences **107**, 17899–17904.

SATHE, A., 2010: Atmospheric stability and wind profile clima-tology over the north Sea-Case study at Egmond aan Zee. – Proceedings of the conference torque, 1–10.

SCHNEEMANN, J., A. ROTT, M. DÖRENKÄMPER, G. STEINFELD, M. KÜHN, 2019: Cluster wakes impact on a far distant off-shore wind farm's power. – Wind Energy Sci. Discus., publsi-hed online. DOI: 10.5194/wes-2019-39.

SIEDERSLEBEN, S.K., 2019: Numerical analysis of offshore wind farm wakes and their impact on the marine boundary layer. – PhD thesis, Universität zu Köln.

SIEDERSLEBEN, S.K., A. PLATIS, J.K. LUNDQUIST, A. LAM-PERT, K. BÄRFUSS, B. CANADILLAS, B. DJATH, J. SCHULZ-STELLENFLETH, J. BANGE, T. NEUMANN, OTHERS, 2018a: Evaluation of a wind farm parametrization for mesoscale at-mospheric flow models with aircraft measurements. – Meteo-rol. Z. **27**, 401–415.

SIEDERSLEBEN, S.K., J.K. LUNDQUIST, A. PLATIS, J. BANGE, K. BÄRFUSS, A. LAMPERT, B. CAÑADILLAS, T. NEUMANN, S. EMEIS, 2018b: Micrometeorological impacts of offshore wind farms as seen in observations and simulations. – Env. Res. Lett., published online, https://iopscience.iop.org/article/10.1088/1748-9326/aaea0b/pdf.

SIEDERSLEBEN, S.K., A. PLATIS, J.K. LUNDQUIST, B. DJATH, A. LAMPERT, K. BÄRFUSS, B. CAÑADILLAS, J. SCHULZ-

STELLENFLETH, J. BANGE, T. NEUMANN, S. EMEIS, 2020: Turbulent kinetic energy over large offshore wind farms observed and simulated by the mesoscale model WRF (3.8.1). – Geosci. Model Develop. **13**, 249–268, DOI: 10.5194/gmd-13-249-2020.

SMEDMAN, A.S., U. HÖGSTRÖM, H. BERGSTRÖM, 1996: Low level jets – a decisive factor for off-shore wind energy siting in the baltic sea. – Wind Engineering **20**, 137–147.

SMEDMAN, A.S., H. BERGSTRÖM, B. GRISOGONO, 1997: Evolution of stable internal boundary layers over a cold sea. – J. Geophys. Res. Oceans **102**, 1091–1099.

SMITH, R.B., 2010: Gravity wave effects on wind farm efficiency. – Wind Energy **13**, 449–458.

STULL, R.B., 2012: An introduction to boundary layer meteorology, volume 13. – Springer Science & Business Media.

TRABUCCHI, D., G. STEINFELD, D. BASTINE, J.J. TRUJILLO, J. SCHNEEMANN, M. KÜHN, 2015: Study of wake meandering by means of fixed point lidar measurements: Spectral analysis of line-of-sight wind component. – J. Phys. Conference Series **625**, 012016.

TRENBERTH, K.E., J.M. CARON, D.P. STEPANIAK, 2001: The atmospheric energy budget and implications for surface fluxes and ocean heat transports. – Climate Dyn. **17**, 259–276, DOI: 10.1007/PL00007927.

TULLOCH, R., K.S. SMITH, 2009: Quasigeostrophic turbulence with explicit surface dynamics: Application to the atmospheric energy spectrum. – J. Atmos. Sci. **66**, 450–467.

VAUTARD, R., F. THAIS, I. TOBIN, F.M. BRÉON, J.G.D. DE LAVERGNE, A. COLETTE, P. YIOU, P.M. RUTI, 2014: Regional climate model simulations indicate limited climatic impacts by operational and planned european wind farms. – Nature communications **5**, 3196.

VEERS, P., K. DYKES, E. LANTZ, S. BARTH, C.L. BOTTASSO, O. CARLSON, A. CLIFTON, J. GREEN, P. GREEN, H. HOLTTINEN, OTHERS, 2019: Grand challenges in the science of wind energy. – Science **366**, eaau2027, DOI: 10.1126/science.aau2027.

VERHOEF, A., M. PORTABELLA, A. STOFFELEN, H. HERSBACH, 2008: CMOD5. n-the CMOD5 GMF for neutral winds. – Technical Report SAF/OSI/CDOP/KNMI/TEC/TN/3, 165, KNMI, De Bilt, Netherlands.

VERMEER, L., J.N. SØRENSEN, A. CRESPO, 2003: Wind turbine wake aerodynamics. – Prog. Aerospace Sci. **39**, 467–510.

VOLKER, P., J. BADGER, A.N. HAHMANN, S. OTT, 2015: The Explicit Wake Parametrisation v1.0: A wind farm parametrisation in the mesoscale model WRF. – Geosci. Model Develop. **8**, 3715–3731.

WANG, C., R.G. PRINN, 2011: Potential climatic impacts and reliability of large-scale offshore wind farms. – Env. Res. Lett. **6**, 025101.

WESTERHELLWEG, A., B. CANADILLAS, A. BEEKEN, T. NEUMANN, 2010: One year of LiDAR measurements at FINO1-platform: Comparison and verification to met-mast data. – In: 10th German Wind Energy Conference, Bremen, 18–19.

WIKLE, C.K., R.F. MILLIFF, W.G. LARGE, 1999: Surface wind variability on spatial scales from 1 to 1000 km observed during TOGA COARE. – J. Atmos. Sci. **56**, 2222–2231.

WU, Y.T., F. PORTÉ-AGEL, 2012: Atmospheric turbulence effects on wind-turbine wakes: An LES study. – Energies **5**, 5340–5362.

XIA, G., M.C. CERVARICH, S.B. ROY, L. ZHOU, J.R. MINDER, P.A. JIMENEZ, J.M. FREEDMAN, 2017: Simulating impacts of real-world wind farms on land surface temperature using the WRF model: Validation with observations. – Mon. Wea. Rev. **145**, 4813–4836.

XU, Y., L.L. FU, R. TULLOCH, 2011: The global characteristics of the wavenumber spectrum of ocean surface wind. – J. Phys. Oceanography **41**, 1576–1582.

ZHOU, L., Y. TIAN, S.B. ROY, C. THORNCROFT, L.F. BOSART, Y. HU, 2012: Impacts of wind farms on land surface temperature. – Nature Climate Change **2**, 539.